



since 1961

Baltica

BALTICA Volume 33 Number 2 December 2020: 146–165

<https://doi.org/10.5200/baltica.2020.2.3>

Distribution of organic matter and evaluation of brittleness index of the Lower Silurian shales of west Lithuania based on interpretation of well logs

Saulius Šliaupa, Jurga Lazauskienė, Saulius Lozovskis, Rasa Šliaupienė

Šliaupa, S., Lazauskienė, J., Lozovskis, S., Šliaupienė, R. 2020. Distribution of organic matter and evaluation of brittleness index of the Lower Silurian shales of west Lithuania based on interpretation of well logs. *Baltica*, 33 (2), 146–165. Vilnius. ISSN 0067-3064.

Manuscript submitted 21 August 2020 / Accepted 16 November 2020 / Published online 22 December 2020

© Baltica 2020

Abstract. There is little known of the basic parameters of the Lower Silurian graptolitic black shales that are considered the most prospective unconventional gas reservoir in west Lithuania, situated in the deep central part of the Baltic sedimentary basin. Hundreds of deep oil exploration wells have been drilled in the area of interest, owing to extensive exploration of oil fields. The lower and middle Llandovery interval was mainly drilled with coring, while most of the section was covered by only logging. Therefore, the knowledge of major parameters of the Lower Silurian shales is rather obscure and is based on scarce rock sample data. The gamma-ray, electrical resistivity and sonic logs were utilised, together with mineralogical studies of rock samples to document vertical and lateral distribution of organic matter. Also, the brittleness index was defined to characterise the whole Lower Silurian section. Some unexpected trends were identified that may redirect exploration strategy in west Lithuania. The combined application of mineralogical studies and well logs indicate a much higher exploitation quality of the Lower Silurian shales than previously believed. A higher organic matter content and brittleness were derived from logging data in the Lower Silurian shales.

Keywords: Baltic basin; sonic; gamma-ray logs; resistivity logs; total organic carbon (TOC); brittleness index

✉ *Saulius Šliaupa* (saulius.sliaupa@gamtc.lt), *Rasa Šliaupienė* (rasa.sliaupiene@gamtc.lt) Institute of Geology and Geography, Nature Research Centre, Akademijos 2 Str., LT-08412, Vilnius, Lithuania, *Jurga Lazauskienė* (jurga.lazauskiene@gf.vu.lt), *Saulius Lozovskis* (saulius.lozovskis@gf.vu.lt), Faculty of Chemistry and Geosciences of Vilnius University, M.K. Čiurlionio Str. 21/27, LT-03101 Vilnius, Lithuania

INTRODUCTION

Lithuania is situated in the Baltic sedimentary basin that is considered a proven hydrocarbon basin and may, also, comprise associating unconventional shale and gas resources. The conventional hydrocarbon reservoirs are related to the Cambrian quartzose sandstones and Ordovician and Silurian limestones (Brančulis *et al.* 1993; Freimanis *et al.* 1993; Zdanavičiūtė, Sakalauskas 2001). The hydrocarbon reservoirs intercalate to the organic-rich shale packages of the same age in the Baltic basin (Poprawa 2010; Jarzyna *et al.* 2017). The shaly succession of the Lower Silurian age is the most prospective tight reservoir in the Bal-

tic sedimentary basin due to considerable thickness and high enrichment in organic matter (OM).

Extensive exploration of shale gas was carried out in adjacent Poland. In Lithuania, the evaluation of the Lower Silurian shales was based mainly on examination of drill core samples, focusing on the characterisation of organic matter (Kanev *et al.* 1994; Zdanavičiūtė, Lazauskienė 2007, 2009; Šliaupa *et al.* 2016). The recent paper by Šliaupa *et al.* (2020) initiated discussions on mechanical and petrophysical properties of Silurian shales of west and central Lithuania, realising that these properties are essential in evaluating exploitation and production characteristics of shales.

GEOLOGY OF THE LOWER SILURIAN OF LITHUANIA

The Silurian sedimentary succession comprises the main part of the sedimentary infill of the Baltic sedimentary basin (Paškevičius 1997). The thickness of the Silurian succession ranges from about 100 m in east Lithuania to about 800 m in south-west Lithuania (Fig. 1). The thickness increases further to the south-west and exceeds 2.5 km in north-westernmost Poland and is about 5 km thick in the highly tectonized Bornholm Graben area (De Vos *et al.* 2010) dissected by the Sorgenfrey-Tornquist zone which is the part of the Trans-European Suture Zone punctuating the western margin of the Baltica continent (Thybo 1997). Burial modelling suggests 5 km subsidence during the Silurian time in north Poland (Botor *et al.* 2019).

The large thickness of the Silurian succession is explained in terms of the flexural loading induced by overthrusting of the East Avalonian microcontinent onto the western margin of the Baltica continent (Lazauskienė *et al.* 2002, 2003; Poprawa *et al.* 1997,

1999). The downflexing of the lithosphere was initiated in the latest Ordovician and climaxed in the latest Silurian. It explains the westward increase in the thickness of the Silurian sediments. Furthermore, the growth of the West European orogen is well reflected in increasing sedimentation rates in the foreland basin from the earliest to the latest Silurian (Fig. 2). In west Lithuania, the sedimentation rate is estimated as low as 6 m/Ma during the Llandovery time, while 300 m/Ma during the Prídolí time. The north-west trending zone is distinct in the Silurian isopach map of west Lithuania. The thickness difference is about 120 m (from ~470 m in the east to ~520 m in the west).

The thickness of the Lower Silurian is about 150 m in west Lithuania. There are little changes in the thickness across Lithuania that is typical of uncompensated sedimentation conditions (Fig. 2). The low influx of the terrigenous material is explained in terms of the incipient orogenic stage of the low-topography of the provenance area. Several lithofacies zones are documented in the Lower Silurian section across Lithuania (Fig. 2). The western part of Lithuania comprises black shales based by several meters thick micritic limestones. Black shales pass to the transition zone of intercalating black and greenish-grey shales in middle Lithuania (Fig. 2). In the East, they are based by the greenish-grey calcareous shales in the lower part of the section. The upper part of the section is more complex. It is represented by dominating limestones that grade to dolomites overlain by alternating sabkha dolomites and gypsum in the eastern periphery of the basin. This marginal zone is embroidered by the regressive belt of small bioherms.

The Upper Silurian succession is of up to 950 m thick (Fig. 2) and is represented by grey mudstones that contain a higher amount of carbonate admixture compared to the underlying Lower Silurian shales. The increasing content of carbonate admixture in shales is likely related to the shallowing of the sedimentation environment driven by the gradually increasing influx of terrigenous material to the basin. In the eastern periphery of the basin, shales give way to carbonaceous rocks (Paškevičius 1997; Lapinskas 2000).

The Lower Silurian succession is composed of the Llandovery and Wenlock black shales. There are no sedimentation breaks documented in the Lower Silurian section in west Lithuania. The Juuru, Raikküla, and Adavere regional stages (RSt) compose the Llandovery Series, while the Jaani, Jagurahu, and Géluva RSts are defined in the Wenlock Series (Paškevičius 1997).

In west Lithuania, several metres thick micritic limestones are attributed to the Juuru RSt that is distinct by the gamma-ray log minimum (Fig. 3). There is a thin transition zone of marlstones and limestones passing upwards to the most gamma-ray active (200-400 API) black graptolitic shales of the Raikküla RSt,

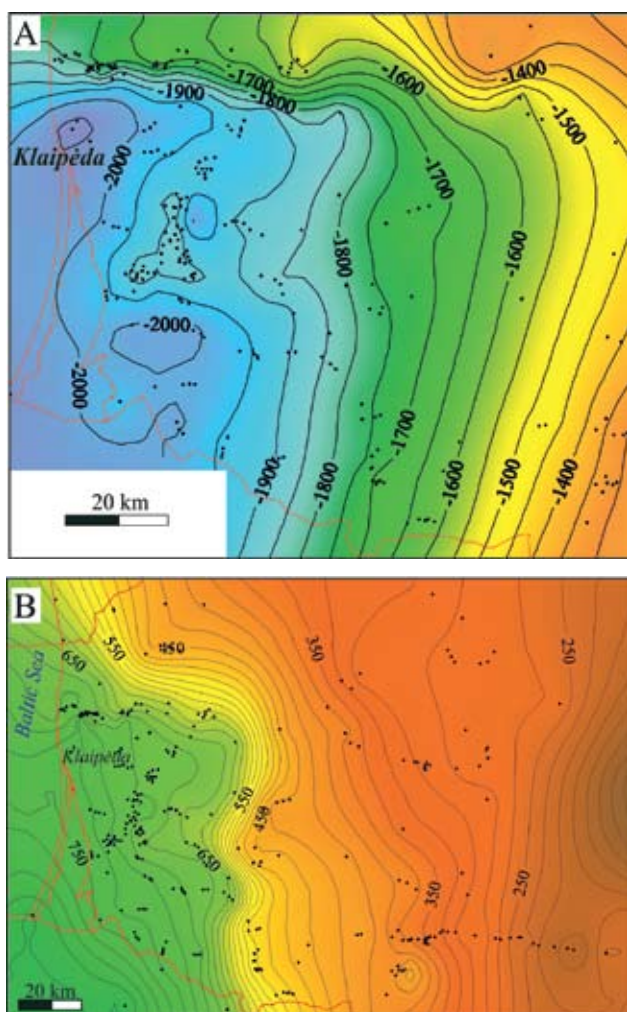


Fig. 1 Depths (bottom, m) and isopach maps of the Silurian succession of west and central Lithuania. No fault tectonic elements are indicated

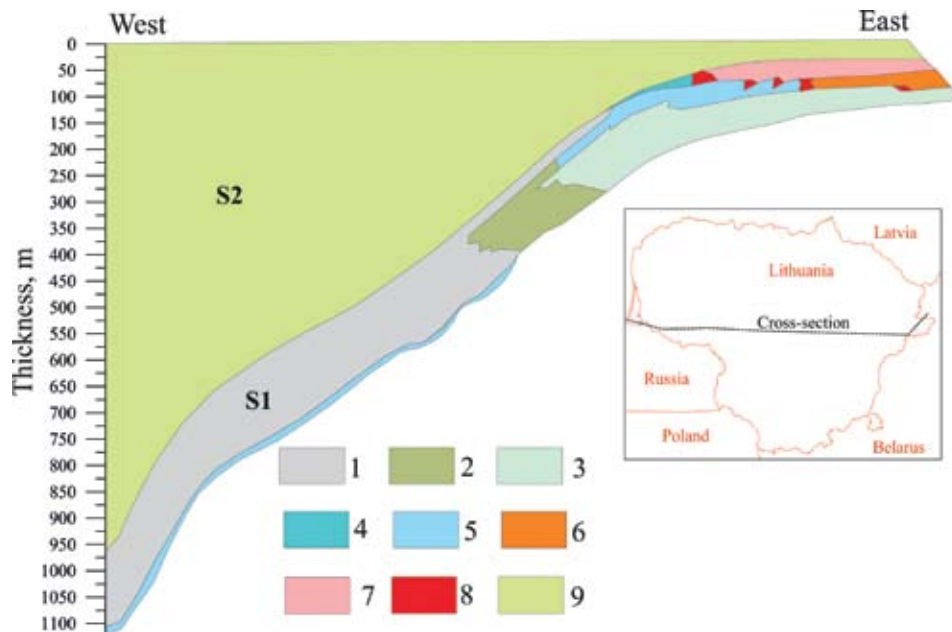


Fig. 2 Geological cross-section of the Silurian succession of Lithuania, west-east. 1 – graptolitic black shales, 2 – black and greenish grey graptolitic shales, 3 – greenish-grey graptolitic shales, 4 – grey shales and limestones, 5 – limestones, 6 – dolomite, 7 – dolomite and gypsum, 8 – bioherms, 9 – Upper Silurian shales and carbonates (not discriminated) (modified after Paškevičius (1997))

the thickness of which ranges from about 4 to 11 m. This remarkable geological layer is overlain by about 40 m thick Adavere RSt black shales, the gamma-ray activity of which varies between 180–200 API. This package shows a slight regression pattern explained by carbonate content increasing upwards.

The Wenlock succession starts with the calcareous black shales attributed to the Jaani RSt. It is about 15 m thick. The overlying Jagurahu RSt indicates

reestablishment of more clayey sedimentation conditions. It is about 60 m thick. The Gėluva RSt shales of about 20 m thick crown the Wenlock succession. The gamma-ray activity of the Wenlock rocks is about 190–210 API.

CHARACTERISATION OF ORGANIC MATTER OF THE LOWER SILURIAN SHALES IN WEST LITHUANIA

There are abundant data published to describe organic matter (OM) of west and middle Lithuania. The most recent studies were published by Zdanavičiūtė and Lazauskienė (2009) and Šliaupa *et al.* (2016). The kerogen is composed of phytoplankton, zooplankton, and bacterial remnants (Zdanavičiūtė, Swadowska 2002). The oil of west Lithuania contains 70–85% of saturated compounds with the predominance of light n-alkanes and is almost devoid of steranes and terpenes (Zdanavičiūtė, Lazauskienė 2009). Pyrolysis analysis indicates a rather low Rock-Eval peak S1, mainly in the range of 0.28–2.88 mg HC/g-rock that points to a low content of trapped HC in the shales (Šliaupa *et al.* 2016). The kerogen is classified as oil-prone Type II.

The thermal maturity of OM is variable in west Lithuania. The oil window (Tmax values >435°C) are defined in most of the territory of west Lithuania (Fig. 4). The area characterised by low Tmax values is considered non-prospective for shale gas exploration. In west Lithuania, two prospective and priority areas can be defined (Fig. 4). The largest priority

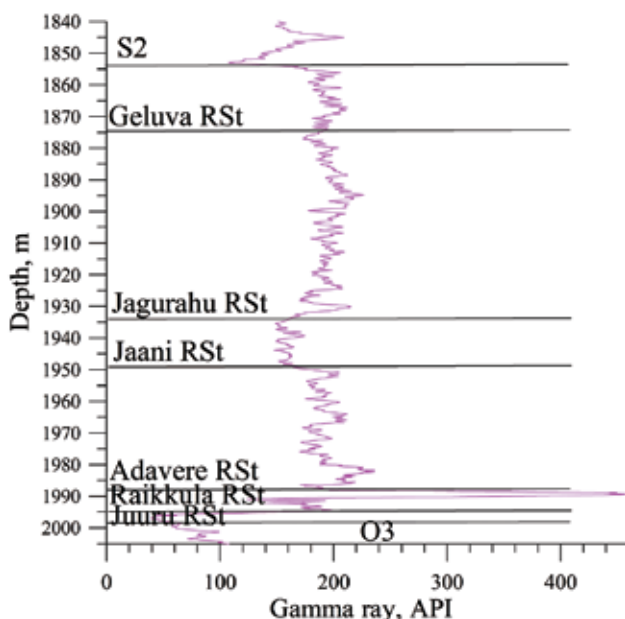


Fig. 3 Gamma-ray log of the lower part of the Silurian section, well Barzdėnai-1, west Lithuania. Regional stages of the Lower Silurian are indicated. O3 shows the top of the Upper Ordovician, S2 is the base of the Upper Silurian

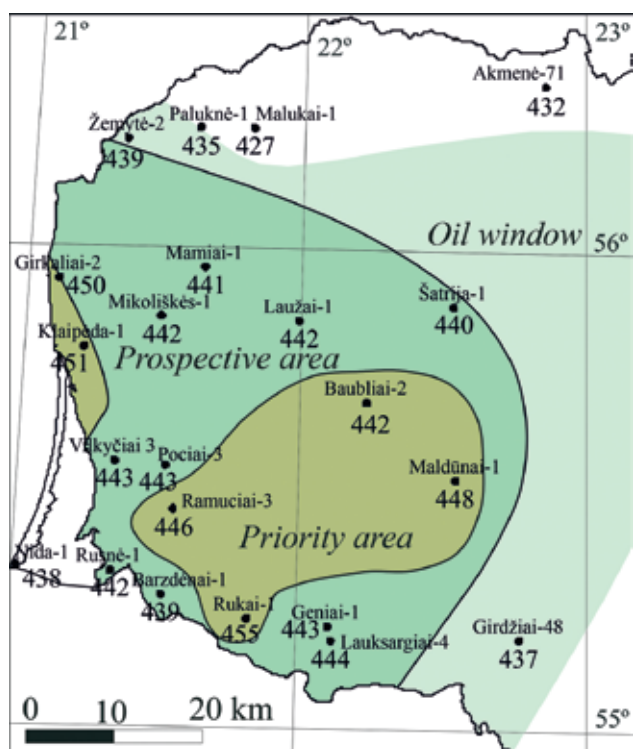


Fig. 4 Prospects of the Lower Silurian shale gas of west Lithuania based on thermal maturity of organic matter (Šliaupa *et al.* 2016). Oil window area, prospective area, and two priority areas are defined. Measured Tmax relates (numbers 427, 432, 435, etc.) to thermal maturity of OM estimated for the Lower Silurian shales

area is situated in the southern part of west Lithuania, where Tmax values vary between 442 °C and 455 °C. Vitrinite-calibrated reflectance was reported as high as 1.01, 1.15 and 1.94 in three shale samples in the southern part of the priority area (wells Rukai-1, Ramučiai-3 and Vainutas-1, respectively) (Zdanavičiūtė, Lazauskienė 2009). Together with Tmax values of 450–455 °C it implies wet gas formation. The second priority area is centred by Klaipėda City. Tmax was measured as high as 450–451 °C there.

The maximum burial of the basin took place in west Lithuania during the latest Devonian-earliest Carboniferous and associated with an episode of the igneous activity reported from the central part of the Baltic Sea (Motuza *et al.* 2015). It was the major stage of hydrocarbon generation in the Baltic sedimentary basin (Šliaupa *et al.* 2002, 2004; Šliaupa, Hoth 2011). The HI (hydrocarbon index) ratio to TOC% classifies the Lower Silurian shales as a poor-to-good HC source. The production index (PI) is, however, rather low, i.e. 0.05–0.13 mg/g TOC (Šliaupa *et al.* 2016).

METHODS AND DATA

XRD measurements were performed in Core Laboratories (<https://www.corelab.com>) and were complemented by measurements carried out at the

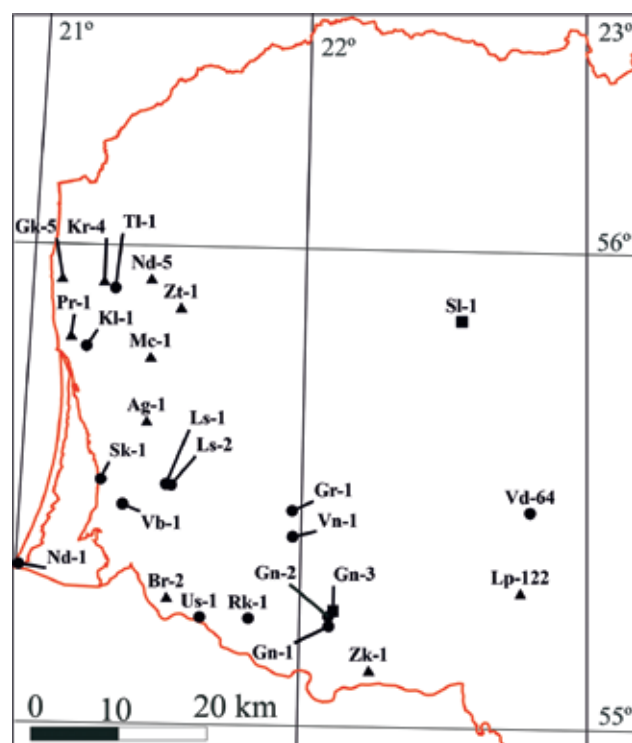


Fig. 5 Location of studied deep wells. Symbols: triangle – interpretation of well logs, black dots – drill core samples, black square – interpretation of well logs and rocks samples. Wells: Ag-1 – Agluonai-1, Br-2 – Barzdėnai-2, Gk-5 – Girkaliai-5, Gn-1 – Geniai-1, Gn-2 – Geniai-2, Gr-1 – Gorainiai-1, Kl-1 – Klaipėda-1, Kr-1 – Kretinga-1, Ls-1 – Lašai-1, Ls-2 – Lašai-2, Lp-122 – Lapgiriai-122, Mc-1 – Maciučiai-1, Nd-1 – Nida-1, Pr-1 – Purmaliai-1, Rk-1 – Rūkai-1, Sl-1 – Slapgiriai-1, Tl-1 – Toliai-1, Us-1 – Usėnai-1, Vd – Vidukė-1, Zt-1 – Žūtautai-1

laboratories of the Centre of Physical Sciences and Technology (Vilnius). The XRD technique was applied to identify the mineral composition of 73 samples collected from fifteen wells (Fig. 5). The quantitative analysis of data was based on a modified methodology proposed by Srodon *et al.* (1992, 2001) and Mystkowski *et al.* (2002). The whole rock mineral identification was based on correspondence of experimental d-values with the diagnostic hkl/reflections from the International Centre for Diffraction Data (1993). Samples were crushed and milled up to <2 μm fraction; 4 ml methanol was used in a ratio of 3 g of a sample. The XRD data were measured on the Bruker X-ray D8 Advance diffractometer; applied voltage was 50 kV with 40 mA current. For non-clay minerals, counting at 2 s per 0.02°2θ step was used, while an additional scan at 5 s per 0.01°2θ step was used for clay minerals at the 59° to 64°2θ range. Empirical calibration curves were used to relate the area of an ‘organic hump’ on an XRD trace to OM content. These curves were calibrated by using XRD patterns of samples that are spiked with an internal standard (Mandile and Hutton 1995).

The mineral composition of the Silurian shale samples was also analysed by adopting the scanning electron microscope QUANTA 250 equipped with an EDS spectroscope (SEM). The 1.0 nA current was used at the voltage of 15–20 kV.

Mineral composition is an important parameter controlling rock brittleness. The mineral brittleness index (MBI) was calculated using several correlation equations relating mineral composition to brittleness. Equations were developed for different regions that show different geological conditions; therefore, some differences between MBI values obtained using different equations should be expected. Two correlation equations are most often used to calculate shale MBI. Jarvie *et al.* (2007) and Wang, Gale (2009) correlation equations developed for Carboniferous Barnett carbonate bounded shales containing 1–3% TOC that is close to Lithuanian Lower Silurian shales. Also, Pachytel *et al.* (2017) published recently a MBI correlation equation for the Lower Palaeozoic shales of north Poland. The aforementioned equations are listed below:

$$\text{MBI} = \frac{\text{Qz}}{\text{Qz} + \text{Ca} + \text{Clay}}, \quad (1)$$

$$\text{MBI} = \frac{\text{Qz} + \text{Dol}}{\text{Qz} + \text{Dol} + \text{Ca} + \text{Clay} + \text{TOC}}, \quad (2)$$

$$\text{MBI} = \frac{\text{Qz} + \text{Dol} + \text{Ca} + \text{Feld} + \text{Plg}}{\text{Qz} + \text{Dol} + \text{Ca} + \text{Feld} + \text{Clay} + \text{Sid} + \text{TOC}}, \quad (3)$$

where (1) is Jarvie *et al.* (2007) equation, (2) is Wang and Gale equation, (3) is Pachytel *et al.* equation. Abbreviations: Ca – calcite, Clay – clay, Dol – dolomite, Feld – feldspars, Qz – quartz, Sid – siderite, TOC – total organic matter.

Well logs are often used as an alternative technique to characterise shales drilled with no coring. The sonic log was performed in eight wells through the whole Lower Silurian interval. These data were interpreted to calculate the log brittleness index (LBI) of shales. The equation proposed for the Carboniferous Barnett shales (Jin *et al.* 2014), Global shale correlation obtained for composite Barnett, Woodford, and Eagle Ford shales (Jin *et al.* 2014), and the equation derived for the Devonian Woodford carbonate bounded shales (Jin *et al.* 2014) were applied in the present study:

$$\text{Barnett} \quad \text{LBI} = -0.01104 \times \text{DTC} + 1.4941, \quad (4)$$

$$\text{Global} \quad \text{LBI} = -0.0142 \times \text{DTC} + 1.7439, \quad (5)$$

$$\text{Woodford} \quad \text{LBI} = -0.012 \times \text{DTC} + 1.4921, \quad (6)$$

where LBI is the log brittleness index (dimensionless), DTC is the sonic wave slowness ($\mu\text{s}/\text{foot}$).

The TOC content was calculated from gamma-ray

logs using the equation developed for west Lithuanian Silurian shales (Šliaupa *et al.* 2016):

$$\text{TOC} [\%] = \exp(0.12 \times \text{GR} [\text{mkr}/\text{h}] \times 0.15). \quad (7)$$

Sonic velocity vs electrical resistivity crossplots are often used to identify the organic-rich intervals, prospective for shale gas exploration (Passey *et al.* 1990). It is also known as the “D log R” method. The baseline correlation of non-source Silurian shales calculated for Lithuanian Silurian shales was defined by Šliaupa *et al.* (2016):

$$d\text{T} = 3522 - 63,102 \times \ln\text{R}, \quad (8)$$

where dT is sonic travel time ($\mu\text{s}/\text{m}$), lnRis natural logarithm of electrical resistivity (ohmm-m).

The slope and intercept of the non-source line are used to calculate a pseudo-sonic log, DtR, from the resistivity log, which can then be plotted on the same scale as the original sonic log. Due to scarceness of available rock samples, the obtained logs cannot be transformed to TOC (%) in west Lithuania. Still, this method provides an effective tool in identification of the relative distribution of OM in the vertical section of the Lower Silurian shales.

RESULTS

Distribution of organic matter in the Lower Silurian shales

The content of OM is a basic parameter in assessing the perspectivity of shales (Wang, Gale 2009; Lu *et al.* 2012). Previous studies of variations of OM content unravelled general vertical and lateral trends in the Silurian succession (Kadūniene 1978, 2001). Total organic carbon (TOC) content is lower than 1% in the Upper Silurian shales (Šliaupa *et al.* 2016), while the Lower Silurian shales have a higher TOC content, exceeding 1.5–2%. The lowest TOC 2% boundary is suggested for prospective shales by Horsfield *et al.* (2008). The close statistical correlation was reported for gamma-ray intensity and TOC content (Šliaupa *et al.* 2016) (Eq. (7)). It enabled continuous mapping of the OM distribution up the Lower Silurian section of wells.

In the present study, this correlation was applied to interpret the logging data of eight wells (Fig. 6). The highest TOC values are modelled in the Raikkūla RSt and exceed 14%. The overlying Adavere RSt and Wenlock shales show minor variations, the average TOC content is about 2%.

A series of maps of the lateral TOC variations was compiled for particular regional stages of the Lower Silurian shales (Fig. 7). Despite different stratigraphic

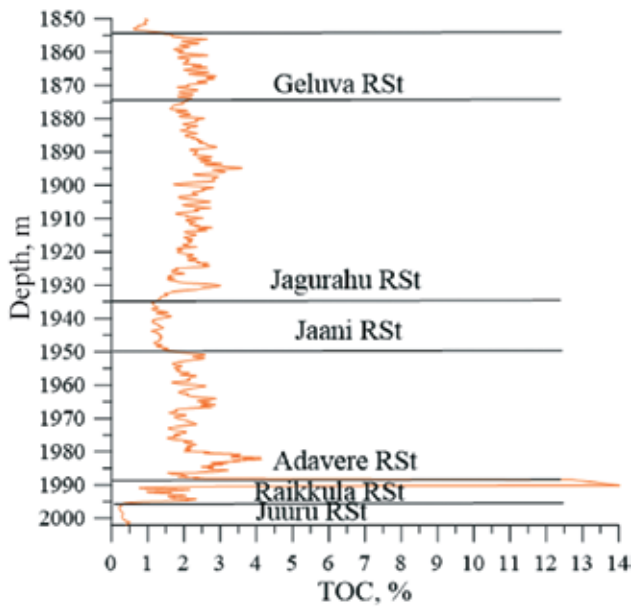


Fig. 6 Example of calculated TOC content in the Lower Silurian shales, well Barzdėnai-1

levels, similar lateral trends are recognised. The maximum content of OM is calculated along the NE-SW trending zone in the eastern part of west Lithuania. The anomalous enrichment in OM is suggested in the southernmost part of this trend (well Žukai-1), averaging 6.64% to 8.88% in particular regional stages. The OM concentration drastically decreases to the east of this zone (well Lapgiriai-122). Also, there is a systematic decrease of OM enrichment to the west. In westernmost Lithuania, TOC values are less than 3%. The lowermost concentration of TOC is calculated in the north-west, TOC concentration is less than 2%.

Gamma-ray intensity is sensitive to variations in the OM content in shales. However, it also strongly depends on clay content. Therefore, an alternative log method should be applied for a more consistent analysis of OM distribution. A combination of the sonic wave travel time log and gamma-ray log can be used to identify relative variations in the OM content.

The Upper Silurian interval is characterised by a

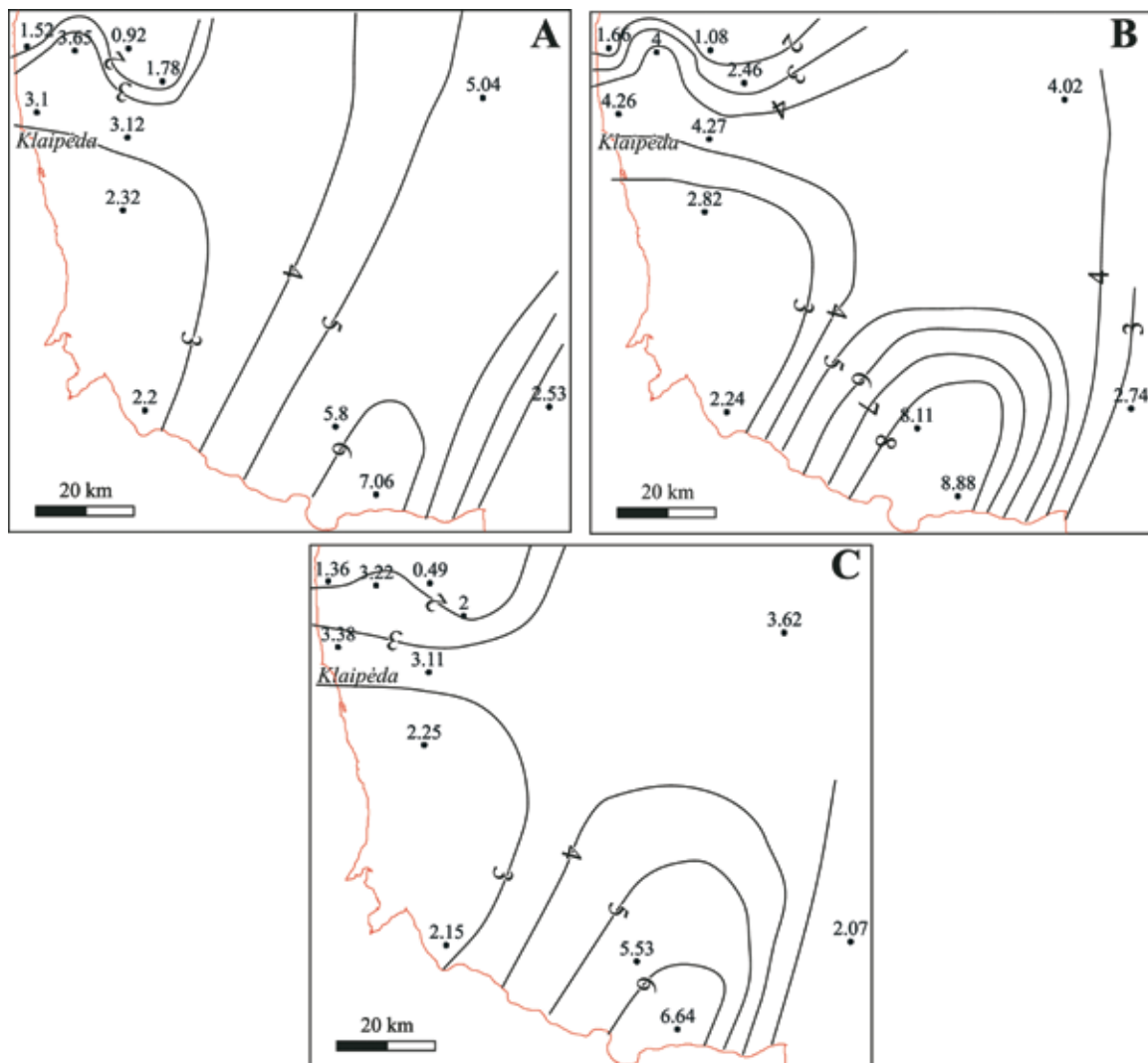


Fig. 7 Lateral distribution of TOC (%) content calculated from gamma-ray log in (A) Adavere RSt, (B) Jagurahu RSt, and (C) Gėluva RSt

high sonic wave travel time in the uppermost part of the section and by a low travel time in the basal part (Fig. 8). This trend is typical of shales that were subject to protracted burial compaction history (Magara 1976; Haesler, Kharitonova 1996; Tassone *et al.* 2014; Baig *et al.* 2016) and reflect decreasing porosity (Athy 1930).

The Lower Silurian part of the section shows the reverse trend, travel time increases with depth, implying that other parameters are crucial for sonic

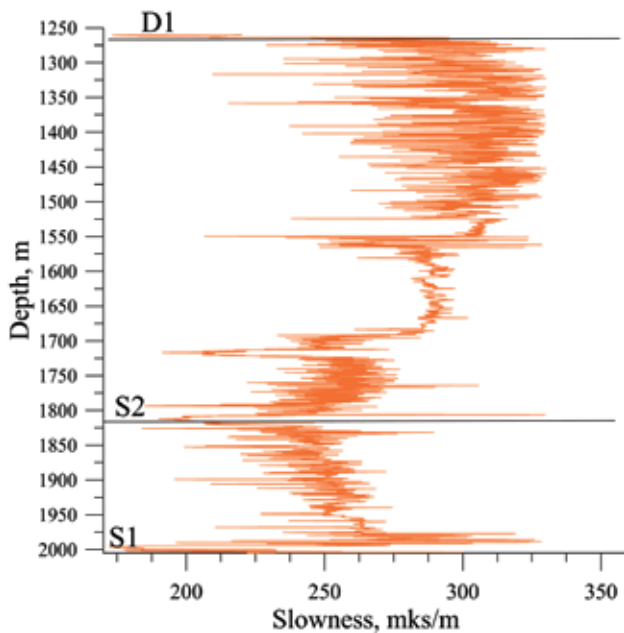


Fig. 8 Sonic travel time in Silurian succession, well Barzdėnai-1, west Lithuania

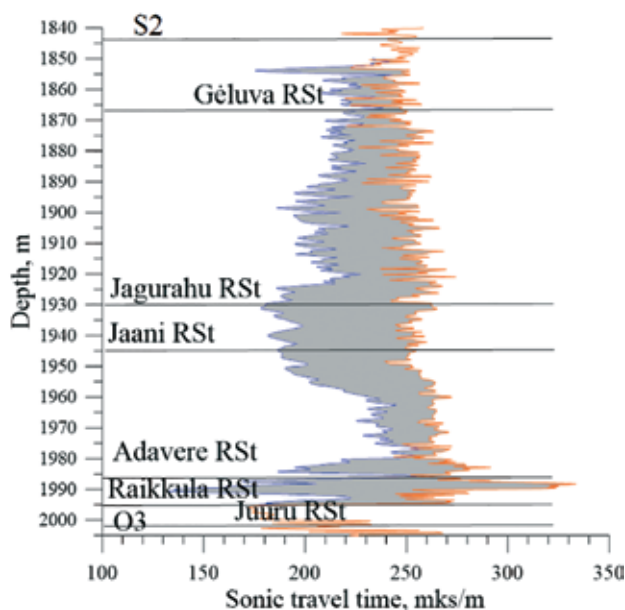


Fig. 9 Sonic transit time log (brown line) calculated based on electrical resistivity log correlation [equation 5] (blue line), well Barzdėnai-1. Stratigraphic subdivision (regional stages of the Lower Silurian) is shown; O3 marks the top of the Upper Ordovician, S2 is the base of the Upper Silurian

wave velocity (Fig. 8). The anomalous wave travel time values are measured in the most organic-rich Raikkula RSt, while gradually decreasing upwards in the overlying shales.

The well Barzdėnai-1 shows considerable deviations between the measured sonic log and DtR calculated using the non-source rock baseline Equation (8) (Figs 9, 10). Generally, the Jagurahu and Gėluva RSts show a systematic decrease in the difference between the two curves suggesting a gradual decrease in OM content upwards. Two “sweet points” are distinct, suggesting the anomalous content of OM at these levels. The most prominent interval is related to the Raikkula RSt which is also well recognised in drill cores. The second organic-rich interval is confined to the Jaani RSt (with the upper and lower transition zones) which, however, has the lowest gamma-ray intensity.

Mineral-based brittleness index of shales

Brittleness is a mechanical rock behaviour under applied stress (Tiryaki 2006) and is pivotal for the development of the unconventional reservoirs. It is notable that this parameter has different definitions depending on the methods applied. Brittleness is the measurement of stored energy before failure and is a function of rock strength, lithology, texture, effective stress, temperature, fluid type, diagenesis, TOC content.

In general, the brittleness index reflects the rock susceptibility to fracturing under applied stress and is an important parameter in tracing prospective inter-

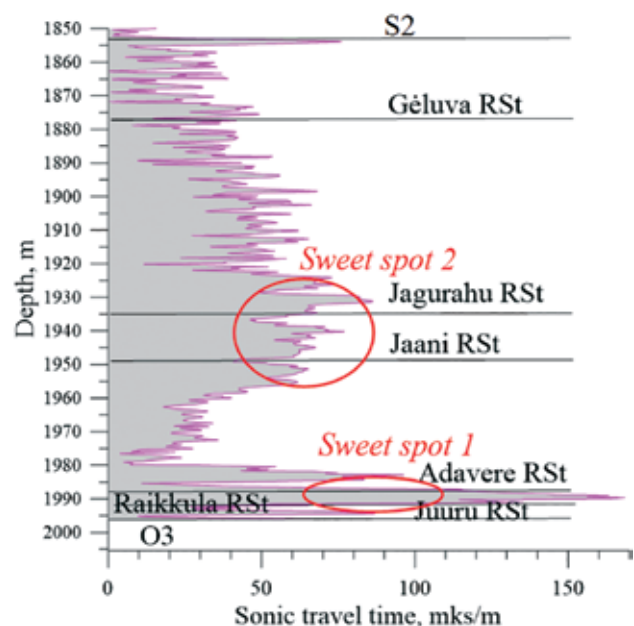


Fig. 10 Misfit between measured and calculated sonic slowness dT and pseudosonic slowness DtR calculated from electric resistivity log. It reflects relative distribution of OM in shales. Stratigraphic subdivision is shown

vals for shale gas exploitation. The brittleness index can be evaluated most consistently using laboratory measurements of the tensile and compressive strength (Altindag 2003). It is, however, of limited application due to difficulty to measure the tensile strength of a shale. Only a few laboratory experiments have been carried out for west Lithuanian Llandovery and Wenlock shales recently (Šliaupa *et al.* 2020).

There are several alternative approaches to characterise rock brittleness. The mineral composition exerts a considerable effect on shale brittleness and is therefore often used in practice. A group of minerals show brittle behaviour under stress, while other minerals react to stress in a ductile manner. There are different correlation equations proposed to calculate the mineral brittleness index (MBI) based on mineral composition (e.g. Jarvie *et al.* 2007; Wang, Gale 2009; Kias *et al.* 2015; Gloriosor, Rattia 2012; Rybacki *et al.* 2016). The west Lithuanian shales were recently evaluated using the mineralogical approach (Šliaupa *et al.* 2020). The other group of methods is based on the evaluation of rock elastic properties. This method was improved to assess shale brittleness of north Poland (Cyz *et al.* 2018).

The mineral composition of shales, mostly of the Raikküla RSt, was defined for 73 samples collected from thirteen oil exploration wells in west Lithuania. XRD technique was applied to identify rock mineral composition (Table 1). It was combined with the SEM (+EDS) petrographic studies of key samples (Fig. 11).

Shales are dominated by clay minerals that average about 55%. Illite (and mixed-layer illite-smectite) composes about 75–80% of the clay mineral fraction. It is most likely of diagenetic nature; illite (with smectite) minerals possibly transformed from mainly detrital smectite that is the most abundant clay mineral in the eastern shallower part of the Silurian Baltic Basin. The second important clay mineral is chlorite which is also a typical mineral for diagenetically transformed clays. Its part ranges mainly between 15% and 20% in the clay fraction. Kaolinite composes only 0.4–4.0% of rock volume.

Quartz grains are abundant in the Lower Silurian shales. The percentage of quartz is about 24–32% (maximum 34%). There is only a minor part of feldspars, which is typical of high chemical weathering of the provenance lithologies. Potassium feldspar predominates over plagioclase, though the opposite ratio is also reported quite often. Quartz grains are of small size and are of rounded and well-rounded shape (Fig. 11). Feldspars are typically partially corroded and that is related to aggressive fluids filling shale pores.

The measured content of carbonates is rather low, as most of the available samples represent organic-rich

shales of the Raikküla RSt. In many cases, carbonate concentration is lower than 5%. However, there is a number of samples that show carbonate content varying between 5% and 25%. Calcite predominates over dolomite at a ratio of 2:1 to 25:1. Only 5 samples show a slight predominance of dolomite. Dolomite is classified mainly as ankerite and contains a high amount of iron. Calcite composes microlithic (mud) aggregates and single crystals, while ankerite grains are of euhedral shape mainly. The latter was possibly formed during the main hydrocarbon generation stage and late diagenetic clay minerals transformation in the Silurian shales.

Pyrite is recognised in a miserable amount in shales. However, it is documented in all studied samples, implying the pervasive formation of this mineral in shales. It composes mainly framboids (early diagenetic) and more rarely is represented in the form of single crystals (late diagenetic). The amount of siderite is lower but is also registered in all examined samples.

As most of the samples were collected from the Raikküla RSt, the measured TOC content is high in examined shales. Its content ranges from 2.5 wt% to 16.3 wt%. Only a few samples are poor in the OM content.

On the shale classification ternary diagram by Gamero-Diaz *et al.* (2013), most of dots cluster in the silica-rich calcareous mudstones field and some are scattered in the mixed argillaceous mudstones field (Fig. 12). Also, there is a wide scatter of dots in the argillaceous siliceous mudstones and mixed mudstones fields. Two dots are classified as a mixed carbonate mudstone. Notably, all dots compose a coherent trend implying a common population (quartz and clay minerals contents decrease with increasing carbonates content).

Rather modest MBI values were calculated using three different Equations (1–3) described above. Calculation results are presented in Table 1. MBI values obtained by using Jarvie *et al.* (2007) and Wang, Gale (2009) correlation equations show little differences and vary mainly in the range of 0.28–0.35 (peak 0.32) and 0.25–0.31 (peak 0.29). As for the north Poland shale equation, MBI values are significantly higher and are as high as 0.35–0.42 with some sub-group of about 0.47.

It is interesting to note that both quartz and feldspars grains content and clay minerals content correlate positively with the MBI (Fig. 13). This correlation is essentially distinct for detrital grains and is less distinct for clay minerals. It implies that detrital grains control mainly the shale brittleness. Clay minerals can accumulate in two ways. They can either aggregate with high-HI (hydrogen index) OM via chemical deposition forming organic-rich laminae, and, alter-

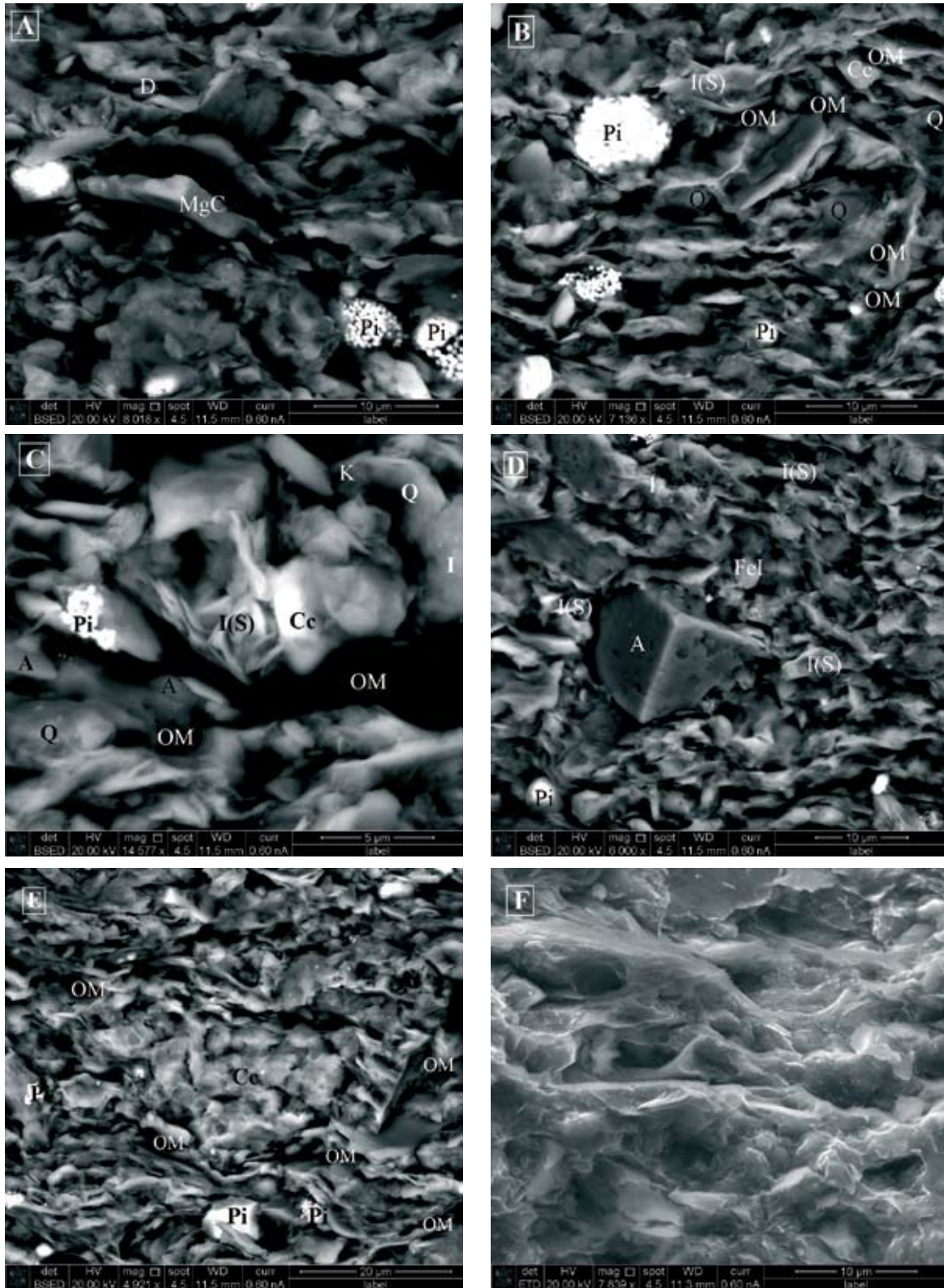


Fig. 11 Backscatter SEM micrograph of sample surface (vertical to bedding), Llandovery shale, depth 2041.9, well Klaipeda-1 (see Table 1 for XRD mineral bulk composition). A – magnesium chlorite (MgC) of well-developed crystalline form in illite with some smectite (I(S)) matrix, with abundant pyrite framboids and very small dolomite crystals; B – illite with some smectite interlayers (I(S)), pyrite framboids and small nodules and abundant silt-size quartz grains, rare small calcite crystals, rich in OM scattered in the clay matrix; C – lath-like illite with smectite I(S) surrounding dissolution pore (former calcite?), with calcite (Cc) and ankerite (A) crystals, small quartz grains, abundant OM, illite (I), scarce kaolinite booklets (K); D – euhedral ankerite (A) in illite (with smectite) I(S) shale; E – micro nodule of micritic calcite (Cc) in illitic (with smectite) shale, with abundant organic matter (OM) and rare pyrite crystals; F – micrograph illustrating low porosity shales (dark openings)

Table 1 Mineral composition (wt%) of the Raikküla RSt shales (several samples are collected from the Upper Llandovery and Wenlock) and calculated MBI values using equations by Jarvie *et al.* (2007), Wang, Gale (2009) and Pachtyel *et al.* (2017) (blue)

Depth (m)	Well	Quartz	K-feldspar	Plagioclase	Calcite	Siderite	Dolomite	Pyrite	Kaolinite	Chlorite	Illite+I-S	TOC	MBI_Jarvie	MBI_Wang_Gale	MBI_Pachtyel
1915.00	Gor-1	30	3	4	2	0.1	1	0.3	2	9	49	0.20	0.33	0.33	0.39
1917.00	Gor-1	29	2	3	7	0.1	4	0.8	2	9	44	5.59	0.32	0.30	0.40
1917.50	Gor-1	31	3	4	6	0.3	1	0.9	5	9	41	7.66	0.34	0.31	0.41
1918.00	Gor-1	30	1	2	8	0.1	0.9	0.6	3	11	44	5.55	0.31	0.30	0.39
1918.60	Gor-1	32	3	3	15	0.2	2	1	2	9	34	8.86	0.35	0.32	0.50
1918.75	Gor-1	16	0.3	1	47	0.1	0.5	0.5	2	5	29	4.49	0.16	0.15	0.61
1919.00	Gor-1	25	1	2	24	0.1	2	0.5	2	8	38	4.90	0.26	0.25	0.50
1920.00	Gor-1	32	4	2	7	0.1	0.7	1	1	10	42	10.10	0.35	0.31	0.42
1920.50	Gor-1	29	4	0.4	3	0.1	0.7	0.7	2	12	49	5.96	0.31	0.29	0.35
1920.75	Gor-1	30	3	0.6	2	0.1	0.7	2	1	10	51	6.45	0.32	0.30	0.34
1921.00	Gor-1	30	2	1	3	0.1	0.6	1	2	8	52	8.53	0.32	0.29	0.34
1921.25	Gor-1	26	4	0.1	15	0.1	1	0.8	0.4	8	45	4.35	0.28	0.26	0.44
1921.75	Gor-1	27	5	0.1	9	0.1	0.5	2	2	7	49	7.69	0.29	0.27	0.38
1922.00	Gor-1	29	4	0.1	7	0.1	0.4	1	2	11	47	7.52	0.30	0.28	0.37
1922.50	Gor-1	31	4	0.5	3	0.1	0.8	2	3	12	44	9.71	0.33	0.30	0.36
1922.80	Gor-1	20	5	2	3	0.1	0.4	3	3	8	36	7.86	0.29	0.26	0.35
1923.50	Gor-1	8	0.9	1	77	0.1	2	0.5	2	3	7	0.13	0.08	0.08	0.88
2041.50	KI-1	29	4	3	17	0.1	1	1	1	9	36	8.53	0.32	0.29	0.49
2041.90	KI-1	29	3	3	2	0.1	2	2	3	12	45	5.44	0.32	0.30	0.36
2042.50	KI-1	26	5	2	3	0.1	3	5	3	12	41	5.88	0.31	0.29	0.37
2043.30	KI-1	33	2	2	7	0.1	1	2	2	10	42	6.80	0.35	0.33	0.42
2043.70	KI-1	29	3	2	6	0.1	0.7	2	2	12	44	8.22	0.31	0.29	0.38
2044.30	KI-1	21	3	2	30	0.4	2	3	3	11	25	5.46	0.23	0.22	0.56
2044.80	KI-1	30	4	3	4	0.1	0.4	1	3	11	45	9.81	0.32	0.29	0.37
2045.30	KI-1	31	2	2	4	0.2	0.7	3	2	12	44	9.10	0.33	0.30	0.37
2046.00	KI-1	27	5	1	10	0.1	0.6	1	1	9	46	8.05	0.29	0.27	0.40
2046.30	KI-1	29	6	2	3	0.1	0.7	3	3	11	44	8.85	0.32	0.29	0.37
2047.25	KI-1	31	6	0.1	2	0.2	1	4	3	7	48	8.07	0.34	0.31	0.37
2047.50	KI-1	34	6	0.2	2	0.3	1	5	3	6	44	8.06	0.38	0.35	0.41
2047.70	KI-1	29	7	1	2	0.1	0.5	4	4	6	47	9.27	0.33	0.30	0.37
2048.25	KI-1	30	5	0.8	0.7	0.2	0.4	8	4	5	47	7.40	0.35	0.32	0.36
2049.00	KI-1	31	6	0.6	2	0.2	1	6	3	7	44	7.22	0.36	0.33	0.39
1984.50	Ls-1	32	5	0.2	0	0.1	0.7	2	1	11	49	2.54	0.34	0.33	0.37
1985.00	Ls-1	29	4	0.3	1	0.1	3	3	1	14	46	3.62	0.32	0.31	0.35
1985.70	Ls-1	30	5	0.6	0.7	0.1	2	2	1	9	51	3.48	0.33	0.32	0.36
1988.50	Ls-1	14	0.4	0.5	64	0.1	0	0.3	1	3	17	0.12	0.14	0.14	0.79
1702.00	SI-1	26	5	3	17	0.4	3	2	4	7	33	15.30	0.30	0.25	0.46
1704.00	SI-1	24	6	2	12	0.1	0.4	1	2	8	44	6.95	0.27	0.25	0.42
1704.80	SI-1	26	4	3	20	0.1	0.6	0.6	3	9	35	3.31	0.28	0.27	0.51
1706.75	SI-1	29	6	3	10	0.2	0.5	3	3	6	41	9.81	0.33	0.29	0.44
1707.00	SI-1	24	5	4	19	0.2	1	1	3	11	33	6.01	0.27	0.25	0.49
1707.75	SI-1	28	5	3	12	0.1	4	1	2	7	39	7.58	0.32	0.29	0.46
1708.50	SI-1	25	4	3	18	0.3	4	1	2	9	35	5.08	0.28	0.27	0.49
1709.00	SI-1	27	5	3	13	0.1	3	1	3	10	36	9.58	0.30	0.27	0.45
1710.60	SI-1	23	5	3	12	0.1	0.9	1	4	12	40	16.30	0.25	0.21	0.37
1711.20	SI-1	24	5	3	14	0.2	1	1	3	9	41	6.49	0.26	0.25	0.44
1929.80	TI-1	17	2	2	40	0.1	1	0.4	0.9	11	27	0.00	0.18	0.18	0.61
1931.20	TI-1	27	5	2	5	0.1	2	2	1	13	42	10.70	0.31	0.27	0.37
1931.50	TI-1	32	5	2	2	0.1	0.7	1	3	10	45	12.00	0.35	0.31	0.37
1932.70	TI-1	29	5	3	8	0.3	1	1	3	10	41	9.06	0.32	0.29	0.42
1932.90	TI-1	29	5	2	9	0.1	0.7	1	2	8	43	8.66	0.32	0.29	0.42

Depth (m)	Well	Quartz	K-feldspar	Plagioclase	Calcite	Siderite	Dolomite	Pyrite	Kaolinite	Chlorite	Illite+I-S	TOC	MBI_Jarvie	MBI_Wang_Gale	MBI_Pachyfel
1933.20	TI-1	27	5	1	10	0.2	2	3	1	9	42	7.66	0.30	0.28	0.42
1933.50	TI-1	26	5	2	22	0.2	1	2	2	8	33	8.78	0.29	0.26	0.51
1933.75	TI-1	31	4	2	7	0.2	1	1	3	10	42	8.82	0.33	0.30	0.41
1934.50	TI-1	31	5	2	5	0.1	0.5	4	3	10	40	10.00	0.35	0.31	0.41
1934.60	TI-1	30	4	3	6	0.1	0.6	1	3	11	42	9.64	0.33	0.30	0.40
1935.00	TI-1	37	5	3	1	0.1	0.2	0.7	4	9	40	15.10	0.41	0.35	0.40
1935.20	TI-1	22	4	2	35	0.5	0.7	0.9	2	6	29	9.56	0.23	0.21	0.57
1935.40	TI-1	31	6	2	10	0.1	0.5	2	3	7	39	10.30	0.34	0.31	0.45
1919.00	Us-1	30	4	5	7	0.2	4	2	0.5	9	40	1.50	0.35	0.34	0.47
1931.50	Us-1	12	0.5	0.8	63	0.1	0.9	0.3	1	5	18	2.66	0.12	0.12	0.74
1932.00	Us-1	22	5	5	4	0.1	2	2	4	13	44	2.72	0.25	0.25	0.36
1934.50	Us-1	26	3	1	14	0.1	3	1	1	8	43	3.82	0.28	0.27	0.44
1935.30	Us-1	28	4	3	7	0.1	1	6	2	6	43	9.84	0.33	0.29	0.41
1935.80	Us-1	26	5	2	10	0.1	0.4	2	2	5	48	7.85	0.29	0.26	0.41
1936.00	Us-1	28	4	0.6	12	0.1	0.6	2	2	6	45	7.56	0.30	0.28	0.42
1937.80	Us-1	29	5	2	8	0.2	0.7	2	2	7	45	8.17	0.32	0.29	0.41
1938.80	Us-1	24	7	0.7	15	0.1	1	3	3	6	42	8.56	0.27	0.24	0.44
2010.00	Vb-1	29	5	1	7	0.1	2	6	2	8	42	10.50	0.33	0.29	0.40
1468.00	Vd-64	26	6	2	9	0.2	1	0.9	3	11	42	15.80	0.29	0.24	0.37
1470.00	Vd-64	23	7	3	12	0.2	1	0.8	3	9	41	11.60	0.26	0.23	0.41
1472.20	Vd-64	27	7	4	13	0.2	0.7	1	4	6	37	15.40	0.31	0.26	0.45

Abbreviation of well names: Gor-1 – Gorainiai-1, Kl-1 – Klaipėda-1, Ls-1 – Lašai-1, Sl-1 – Šlapgiriai-1, TI-1 – Toliai-1, Us-1 – Usėnai-1, Vb-1 – Vabalai-1, Vd-64 – Viduklė-1.

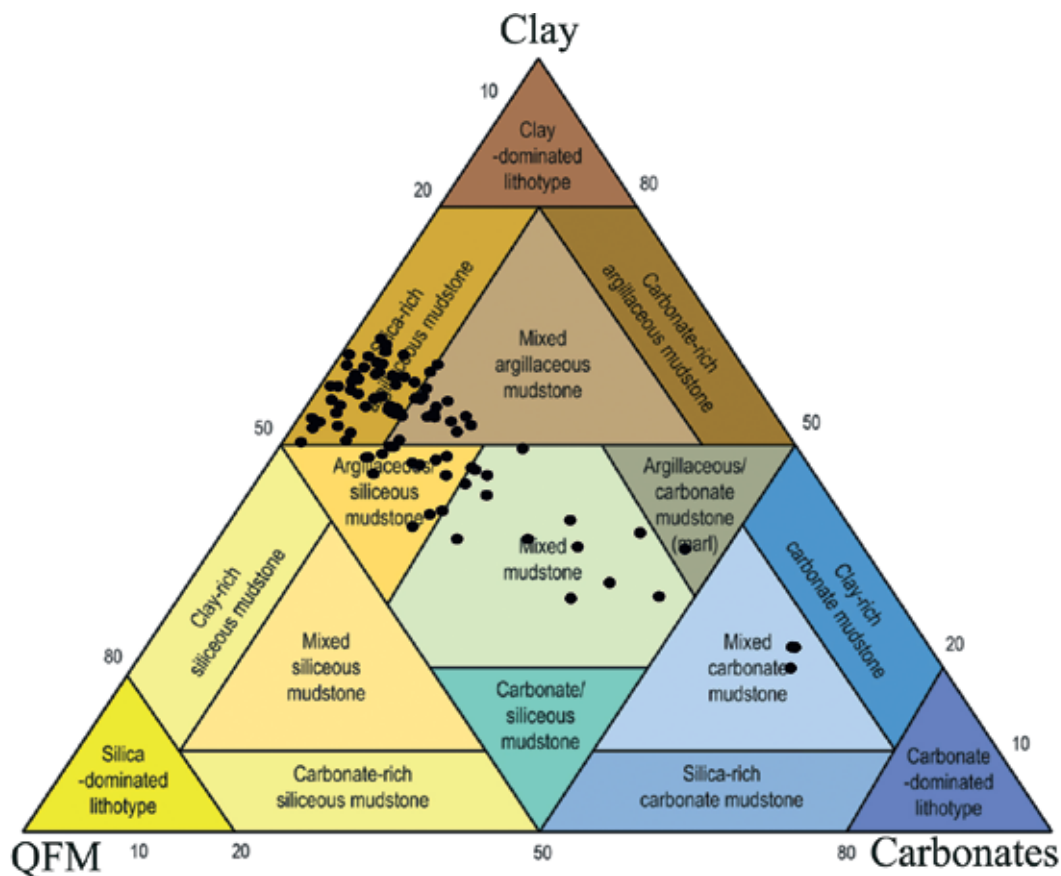


Fig. 12 Core lithological classification for organic-rich mudstones (Gamero-Diaz *et al.* 2013). Data of the west Lithuanian Lower Silurian shales are plotted

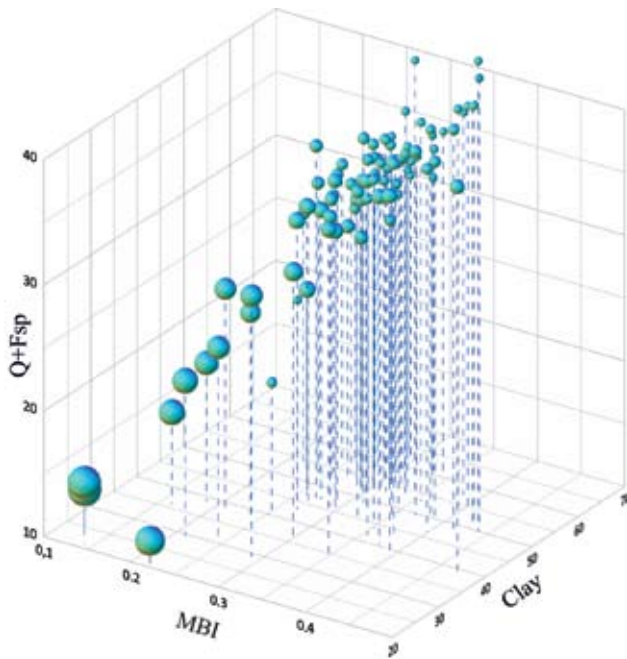


Fig. 13 XYZ graded plot of mineral composition vs MBI (calculated by Woodford equation). Symbols size indicates the relative content of calcite and dolomite in the sample

natively, they can be deposited together with low-HI OM via physical deposition also forming clay-rich shales. Taking into consideration a high HI index of the Lower Silurian OM (219–571 mg HC/gTOC), the former mechanism is more likely. Carbonates have a pronounced diverse correlation with both aforementioned mineral groups (Fig. 13). As they associate with a high HI OM, it suggests the organic origin of carbonates.

Brittleness index calculated from sonic logs

Gas shales are characterised by low matrix permeability. Therefore, hydraulic fracturing should be used to achieve commercial production rates (Sondergeld *et al.* 2010). Commonly, the only limited amount of rock samples is available for analytical studies to derive different rock parameters. In Lithuania, only the Juuru RSt (limestones) and Raikküla RSt (most organic-rich black shales) are well represented by drill core material, while the major part of the Lower Silurian section remains scarcely studied. As explained above, fractured limestones of the Juuru RSt were considered the second potential conventional HC reservoir in west Lithuania and therefore were drilled through with rock sampling.

Equations [4–6] were applied to calculate the log brittleness index. Regardless of an equation applied, there is a clear trend of general increase of the LBI upwards the section (Fig. 14). The Juuru RSt limestones have maximum LBI values. The Raikküla RSt organic-rich shales have average brittleness similar to

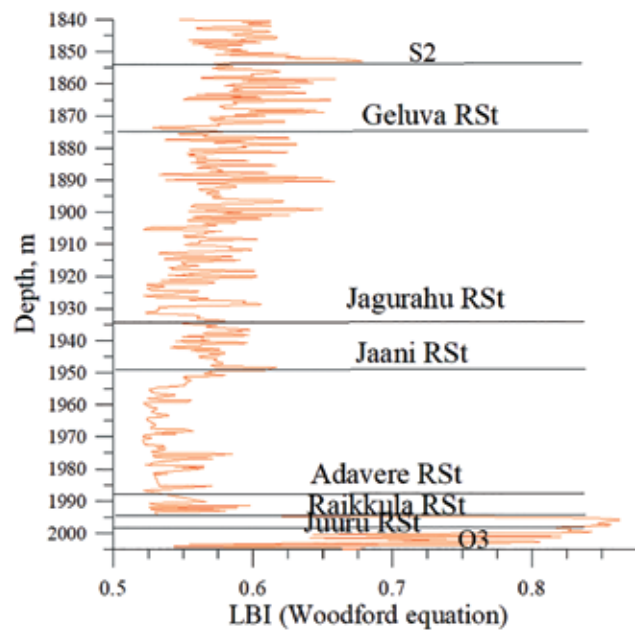


Fig. 14 Log brittleness index calculated using correlation estimated for Woodford shales, well Barzdėnai-1. Log spikes are caused by technical (electrical) disturbances in the logging equipment system

the Adavere RSt black shales. The latter show either no-trend LBI values or a slight upward increase in brittleness. The Jaani RSt shales have increased brittleness. The shales of the Jagurahu and Gėluva RSts grow more brittle upwards.

Interpretation of logging data was averaged to the particular regional stages to identify lateral variations of the LBI in west Lithuania (Tables 2–4). The Raikküla RSt shales have the relatively lowest LBI compared to the overlying shales. However, the Adavere RSt shales are less brittle in some wells (Šlapgiriai-1, Lapgiriai-122, Nausodis-5, Žutautai-1). The Jaani RSt and Gėluva RSt shales have the relatively highest LBI. The Jaani RSt represents a particular layer of increased brittleness, while the Gėluva RSt crowns the Lower Silurian succession characterised by an upward increase of the LBI. Concerning applied equations, the relatively highest LBI values were calculated using the equation developed for Barnett shales, though they are rather close to the LBI calculated by the Global shale correlation equation, the LBI varies from 0.48 to 0.72. The Woodford equation results in relatively lower LBI values.

Three LBI maps were compiled for the Jaani, Adavere, and Jagurahu RSts to illustrate the lateral pattern of shale brittleness. The same trends are recognised for all stratigraphic levels regardless of the correlation equation applied. The LBI systematically increases westward from 0.39 in the east to more than 0.55 in the west (Fig. 14). Furthermore, there is a clear impact of the regional-scale W-E trending Telšiai fault zone of about 200 m amplitude (not in-

Table 2 Average LBI (Barnett shale correlation equation (4)) of the Lower Silurian shales in different wells

Stage	Gėluva RSt	Jagurahu RSt	Jaani RSt	Adavere RSt	Raikkūla RSt
Šlapgiriai-1	0.55	0.52	0.54	0.48	0.57
Barzdėnai-1	0.67	0.64	0.64	0.59	0.57
Kretinga-4	0.59	0.58	0.59	0.54	0.48
Macuciai-1	0.63	0.63	0.64	0.59	0.50
Purmaliai-1	0.68	0.67	0.68	0.64	0.57
Agluonėnai-1	0.67	0.66	0.67	0.64	0.53
Geniai-3	0.56	0.53	0.55	0.5	0.49
Girkaliai-5	0.61	0.60	0.61	0.58	0.53
Lapgiriai-122	0.53	0.52	0.54	0.48	0.52
Nausodis-5	0.68	0.66	0.81	0.65	0.67
Žukai-1	0.57	0.55	0.56	0.49	0.56
Žutautai-1	0.57	0.7	0.63	0.69	0.80

Table 3 Average LBI (Global shale correlation equation (5)) of the Lower Silurian shales in different wells

Stage	Gėluva RSt	Jagurahu RSt	Jaani RSt	Adavere RSt	Raikkūla RSt
Šlapgiriai-1	0.53	0.50	0.51	0.44	0.56
Barzdėnai-1	0.68	0.65	0.65	0.58	0.56
Kretinga-4	0.58	0.57	0.59	0.52	0.44
Macuciai-1	0.64	0.63	0.64	0.59	0.47
Purmaliai-1	0.69	0.68	0.69	0.64	0.56
Agluonėnai-1	0.69	0.67	0.68	0.64	0.51
Geniai-3	0.55	0.5	0.53	0.47	0.46
Girkaliai-5	0.61	0.6	0.61	0.57	0.5
Lapgiriai-122	0.51	0.49	0.51	0.45	0.49
Nausodis-5	0.70	0.67	0.87	0.66	0.68
Žukai-1	0.55	0.53	0.54	0.46	0.55
Žutautai-1	0.55	0.72	0.63	0.71	0.86

Table 4 Average LBI (Woodford shale correlation equation (6)) of the Lower Silurian shales in different wells

Stage	Gėluva RSt	Jagurahu RSt	Jaani RSt	Adavere RSt	Raikkūla RSt
Šlapgiriai-1	0.47	0.44	0.45	0.39	0.49
Barzdėnai-1	0.59	0.56	0.56	0.51	0.49
Kretinga-4	0.51	0.50	0.51	0.46	0.39
Macuciai-1	0.56	0.55	0.56	0.51	0.41
Purmaliai-1	0.60	0.60	0.60	0.56	0.49
Agluonėnai-1	0.60	0.59	0.59	0.56	0.45
Geniai-3	0.48	0.44	0.47	0.41	0.4
Girkaliai-5	0.53	0.52	0.53	0.50	0.44
Lapgiriai-122	0.45	0.43	0.45	0.39	0.43
Nausodis-5	0.61	0.59	0.75	0.58	0.59
Žukai-1	0.49	0.47	0.47	0.41	0.48
Žutautai-1	0.48	0.62	0.55	0.62	0.74

licated on the maps). Shales are less brittle on the northern hanging wall of the fault compared to shales of the foot-wall.

The westward increase in the LBI correlates with the increase of the compaction rate of shales in the same direction and with burial depth (depths of the bottom of the Lower Silurian succession vary from 1435 m in the well Lapgiriai-122 to 2085 m in the well Klaipėda-1). As a result of increasing compaction and associating pore space reduction, the average sonic wave slowness increases (velocity decreases) with decreasing depth (Fig. 15). The sonic wave slowness averages 290 $\mu\text{s}/\text{m}$ in the shallowest Lapgiriai-122

well, while it is about 245 $\mu\text{s}/\text{m}$ in the deepest well Purmaliai-1.

DISCUSSION

The Lower Silurian black shales are about 150 m thick in west Lithuania. It evidences a low sedimentation rate during the sediment-starved basin stage. The lower part (about 5–10 m thick) of the Llandovery Stage is most enriched in OM. It suggests dramatic environmental changes at the Ordovician and Silurian boundary. This boundary is globally marked by the end-Ordovician extinction event (second largest of

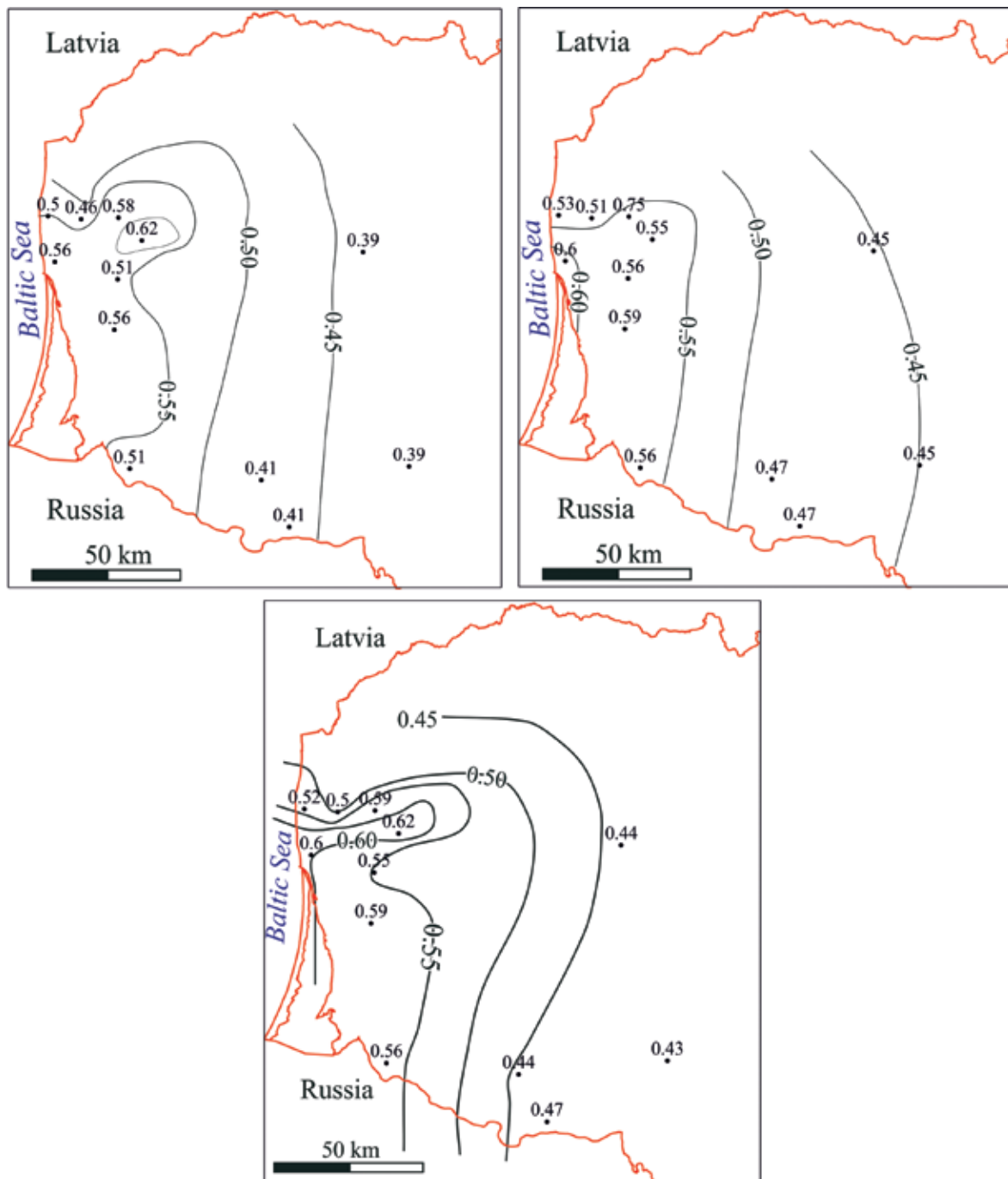


Fig. 15 Log brittleness index calculated using correlation estimated for Woodford shales, well Barzdėnai-1. Log spikes are caused by technical (electrical) disturbances in the logging equipment system

the five mass extinctions of the Phanerozoic), and the Early Silurian post-extinction recovery. Potentially, waters bearing metal ions and other substances toxic to organisms were advected upward into the ocean mixed layer during the glacial maximum. The Upper Ordovician is represented by marlstones and limestones that were replaced by the global sedimentation of the organic-rich black shales during the Early Silurian (Knoll, Holland 1995). There are abundant palaeovalleys filled by limestone debris in the uppermost Ordovician, some of them with oil shows

in middle Lithuania (Laškovas 2002). It is related to the growth of the latest Ordovician Saharan (West African-Amazonian) ice sheet that covered a large part of the Gondwana continent at that time (Delabroye, Vecoli, 2010; Finnegan 2011; Moreau 2011). The oceanic water was 5° C cooler during glaciation and grew warmer during deglaciation. It changed the global ocean circulation during the Early Silurian. Two types of deep ocean circulation could be distinguished: Halothermal Circulation (HTC), involving the formation of Warm Saline Deep Water (WSDW)

in the tropics, promotes anoxia, while Thermohaline Circulation (THC), characterised by Cold Deep Water (CDW) formed at high latitudes, ventilated the deep ocean (Horne 1999) (Fig. 16). The western margin of the Baltica continent was open to the Iapetus Ocean (Caledonian orogen was only at the incipient stage of formation) at the beginning of the Silurian time. Post-glaciation triggered the intense accumulation of OM on the slope of the continent (Fig. 17). It explains a high content of OM in the Lower Silurian shales.

The Raikküla RSt shales are most enriched in OM. They are compatible (Šliaupa *et al.* 2020) to “hot” shales of North Africa and Arabian Peninsula (Belaid *et al.* 2009; Loydell *et al.* 2013). The maximum production of OM is recorded at the beginning of the melting of the ice sheet in the Gondwana continent. Accompanied by an early Silurian global sea level rise, a large amount of OM reached the shallower water platform, as demonstrated by a wide distribution of the black shales on the platform. The newly forming West European orogen represented a barrier facilitating the accumulation of OM on the continental slope. Reradiation of marine communities commenced during the *P. acuminatus* zone (Berry 1987) time that is defined in the basal part of the Juuru RSt (Paškevičius 2019). The $\delta^{13}\text{C}$ isotope values of the Juuru RSt limestones range from -0.5 to +2.5, while Hirnantian limestone $\delta^{13}\text{C}$ isotope values are mainly +4.5 to +7.5 in adjacent Estonia and Latvia (Brenchley *et al.* 2003).

The application of the gamma-ray logs considerably improves the model of distribution of OM in the Lower Silurian shales in west Lithuania. An anomalous zone striking NE-SW was defined, while a lower OM content is suggested in westernmost Lithuania.

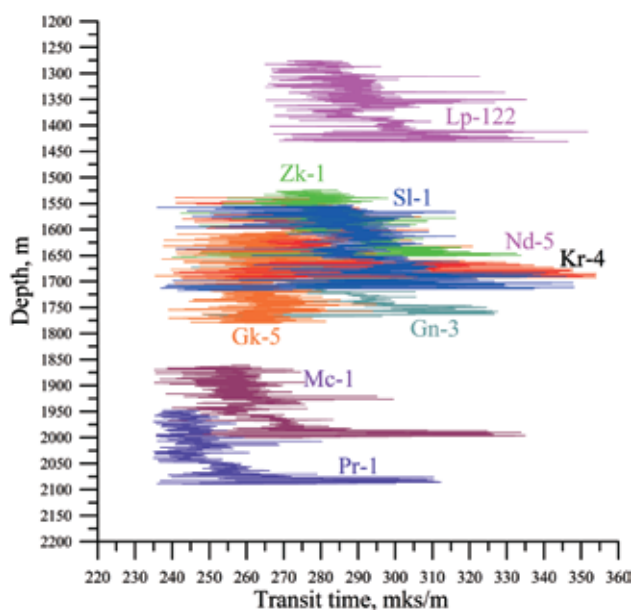
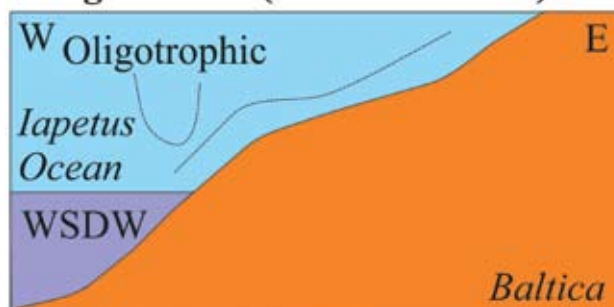


Fig. 16 Composite graphic of sonic transit time vs depth of west Lithuanian wells (see Fig. 5 for wells locations)

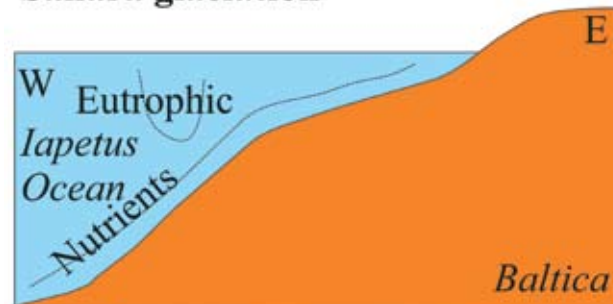
The pattern of OM roughly reflects the thickness variations of the Lower Silurian sediments (Fig. 18). The anomalous OM belt is confined to the Pagėgiai–Šaukėnai trend of increased thicknesses (140–200 m), while the west Lithuanian OM minimum marks the Barzdėnai–Šatrija trend of decreased thicknesses (120–160 m). It can be therefore suggested that those thickness undulations mark long-wavelength tectonic structures active during the Lower Silurian sedimentation. Accordingly, more organic-rich mud accumulated on the basin bottom in the bottom depressions compared to the elevations.

It is interesting to note that increased rates of OM sedimentation are also suggested along the southern (relatively subsided) flank of the regional-scale Telšiai fault striking W–E. It is an important message, because the main stage of the vertical displacement of the Telšiai fault took place during the latest Silurian-earliest Devonian (Stirpeika 1999), owing

Pre-glaciation (stratified ocean)



Sahara glaciation



Post-glaciation

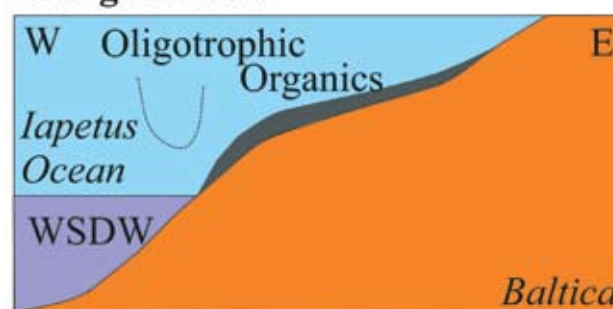


Fig. 17 Illustration of differences in oceanic circulation and productivity during glacial and non-glacial phases (modified after Brenchley *et al.* (1995) and Horne (1999))

to the collision of the Laurentia and Baltica continents (Šliaupa 1999; Šliaupa *et al.* 2000; Poprawa *et al.* 2006). Distribution of OM along the Telšiai zone persuades some early (prefaulting) tectonic activity of the Telšiai fault. It should be noted that this fault zone, defined in the sedimentary cover, is confined to the prominent shear zone in the Palaeoproterozoic basement (Šliaupa 2002).

Yet, application of the gamma-ray logs for the assessment of OM distribution has some inconsistencies. For a better control of the gamma-ray interpretation results, sonic and electrical resistivity logs were used. As it was expected, the well-known Raikküla RSt organic-rich shale was defined as the most distinct organic-rich formation. The distribution of OM in the overlying Lower Silurian shales shows an unexpected trend suggesting the common sedimentation cycle of organic matter. The content of OM reaches the maximum in the Jaani RSt and shows gradual decrease in content upwards and downwards. The Jaani RSt has the lowest gamma-ray intensity in the Lower Silurian section that suggests decreased content of clay minerals in shales. The minimum gamma-ray activity is best explained by the increased content of carbonates. Untypically, it associates with increase in OM accumulation rate. This increase does not necessarily reflect sea level fluctuations. More reasonably,

it is an indication of variations in climate conditions. As regards the lateral distribution, some unexpected trend was defined in west Lithuania. In general, the average values of TOC exceed 2% and that is classified as “excellent” for shale gas prospects (Peters 1986; Dembicki 2017).

The brittleness index depends on several parameters, of which porosity and mineral composition are the most important ones. Rather high values of the MBI were calculated, mainly 0.25–0.35. This is classified as less ductile and less brittle shale according to Perez and Marfurt (2013). After the classification by Wójcicki *et al.* (2017), this is below the lower boundary of prospective shales. The correlation equation developed for north Polish Lower Palaeozoic shales gives higher values, most of samples show the MBI higher than 0.4 and therefore they are plotted above the lower MBI boundary. The main reason for a low brittleness of studied shales is related to a high content of clay minerals and OM (50–60% and 2.5–16.2%, respectively) in studied samples. These shale constituents are the main controlling parameters of shale ductility (Yasin *et al.* 2017). It should be stressed, however, that almost all studied samples were collected from the most organic-rich Raikküla RSt shales, while most of the Lower Silurian section was commonly drilled with no core sampling. Therefore, there might be erroneous understanding of low brittleness of the whole Lower Silurian section.

The application of sonic logs increased considerably the knowledge of this basic exploitation parameter of the Lower Silurian shales. Interpretation of sonic logs suggests that shales overlying this particular Raikküla RSt formation should be classified as less brittle, but mainly brittle (LBI >0.48, after Perez, Marfurt 2013). There is a common trend of increase of the brittleness index upwards in the Lower Silurian section. Most likely, it results from increasing carbonate content upwards. LBI difference between the eastern part of west Lithuania and westernmost Lithuania is about 0.15, and that corresponds to about 650 m burial depth difference. Shale compaction, which relates to porosity, is the main parameter controlling this lateral trend. As it was reported by Šliaupa *et al.* (2020), the measured porosity of the Llandovery shales decreases westwards. The other feature that is clearly defined on LBI maps is the regional Telšiai fault zone. The shales of the hanging wall have lower brittleness, and the average amplitude of this fault zone is 200 m.

CONCLUSIONS

The application of the gamma-ray, sonic and electrical resistivity logs considerably improved the model of perspective of the Upper Silurian gas shales of

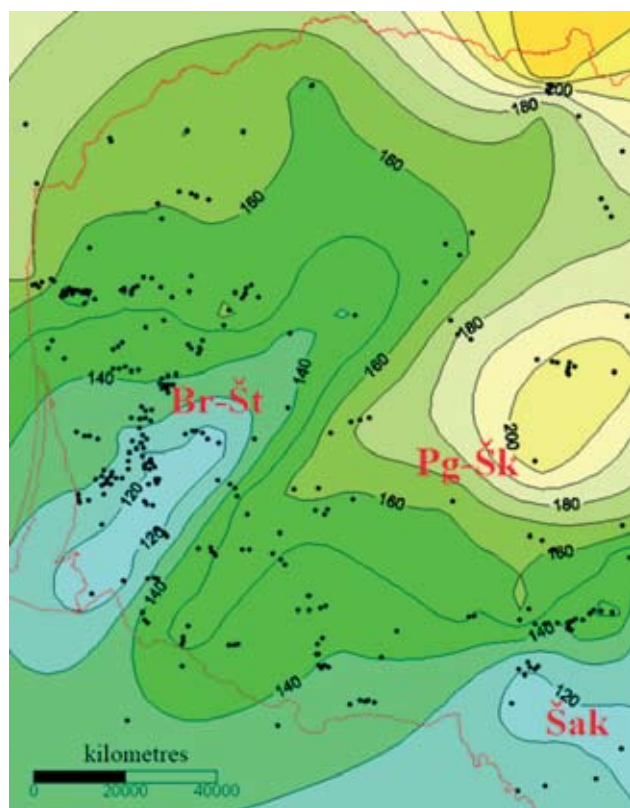


Fig. 18 Isopach map of the Lower Silurian succession. Structures (names according to key wells): Br-Št – Barzdėnai-Šatrija uplift, Pg-Šk – Pagėgiai-Šaukėnai depression, Šak – Šakiai uplift

west Lithuania. So far, the main knowledge of shale properties, such as vertical and lateral distribution of OM and BI was derived from abundant sample data which, however, cover only a very limited stratigraphic interval of the Upper Silurian shales, *i.e.* the organic-rich Raikküla RSt graptolitic black shales. It is only about 15 m thick basal interval of a much thicker (120–200 m) organic-enriched shales package of the Lower Silurian.

As samples were collected mainly from the most organic-rich Raikküla RSt, the calculated mineral brittleness index (MBI) is relatively low and shales are classified as less ductile and less brittle and are below the minimum limit of 0.40 recommended for the potential gas shales. It relates to a high content of ductile constituents like clay minerals and OM in the lowermost Silurian shales. The interpretation of sonic and electrical resistivity logs shows, however, that most of the Upper Silurian shales have LBI of 0.40–0.55 and higher. Shales grow more brittle westward and that is accounted for increasing compaction of shales with increasing depth and associated decreasing porosity. The average LBI difference between the eastern part of the study area and westernmost Lithuania is about 0.15 and that relates to depths difference of 650 m. It is notable that the regional-scale Telšiai fault is well recognised on the LBI maps implying relatively lower brittleness on the hanging wall of the fault. It also suggests pre-faulting tectonic activity of this zone.

The other crucial parameter defining perspective of shales is enrichment in OM. Similar to the MBI, most of available rock samples were collected from the lower part of the Llandovery. The content of OM is therefore high, ranging from about 4% to 20%. Few available samples from the overlying shales show TOC content of about 2% and that is the critical value for gas shales. The interpretation of gamma-ray logs shows, however, a more complex TOC pattern. An anomalous zone trending NE-SW was defined in the eastern part of west Lithuania. Here, the average TOC content ranges from 4–5% to 8.9% in the Jagurahu RSt shales. Unexpectedly, the content of OM decreases to the west and is only about 2% in the westernmost Lithuania. The anomalous belt is roughly confined to the increased thicknesses of the Lower Silurian deposits (interpreted as the Pagėgiai–Šaukėnai sea bottom depression). The vertical pattern of OM also unravelled intriguing trends in particular wells. Electrical resistivity and sonic velocity logs were used. As expected, the most organic-rich formation is related to the Raikküla RSt of about 4–10 m thick. Yet, the second sweet spot has been identified in the Jaani RSt that is characterised by depletion in clay minerals. It, therefore, has high brittleness and can be considered a priority unit in shale gas exploration.

The combined application of mineralogical stud-

ies and well logs indicate a much higher exploitation quality of the Lower Silurian shales than previously believed.

ACKNOWLEDGMENTS

The research was partially supported by the Research Council of Lithuania (a grant within project No TAP LB 06/2013). We thank two anonymous reviewers for their careful reading of the manuscript and their many insightful comments and suggestions.

REFERENCES

- Altindag, R. 2003. Correlation of specific energy with rock brittleness concepts on rock cutting. *Journal of the Southern African Institute of Mining and Metallurgy*, 103, 163–171.
- Athy, L.F. 1930. Density, porosity, and compaction of sedimentary rocks. *American Association of Petroleum Geologists Bulletin*, 14, 1–24.
- Baig, I., Faleide, J.I., Jahren, J., Mondol, N.H. 2016. Cenozoic exhumation on the southwestern Barents Shelf: estimates and uncertainties constrained from compaction and thermal maturity analyses. *Marine and Petroleum Geology*, 73, 105–130, doi: 10.1016/j.marpetgeo.2016.02.024.
- Belaid, A., Krooss, B.M., Littke, R. 2009. Thermal history and source rock characterization of a Paleozoic section in the Awbari Trough, Murzuq Basin, SW Libya. *Marine and Petroleum Geology*, 27, 612–632.
- Berry, W.B. 1987. The Ordovician-Silurian boundary: new data, new concerns. *Lethaia*, 20 (3), 189–291.
- Botor, D., Golonka, J., Anczkiewicz, A.A., Dunkl, I., Papiernik, B., Zajac, J., Guzy, P. 2019. Burial and thermal history of the lower Palaeozoic Petroleum source rocks at the SW margin of the east European craton (Poland). *Annales Societatis Geologorum Poloniae*, 89, 121–152, doi: 10.14241/asgp.2019.12.
- Brangulis, A.P., Kanev, S.V., Margulis, L.S., Pomerantseva, R.A. 1993. Geology and hydrocarbon prospects of the Palaeozoic in the Baltic region. In: Parker, J.R. (ed.) *Petroleum geology of Northeast Europe. Proceedings of the 4th conference*, Geological Society, London, March–April 1992.
- Brenchley, P.J., Carden, G.A.F., Marshall, J.D. 1995. Environmental changes associated with the first strike of the Late Ordovician mass extinction. *Modern Geology*, 20, 69–82.
- Brenchley, P.J., Carden, G.A., Hints, L., Kaljo, D., Marshall, J.D., Martma, T., Meidla, T., Nölvak, J. 2003. High-resolution isotope stratigraphy of Late Ordovician sequences: constraints on the timing of bio-events and environmental changes associated with mass extinction and glaciation. *Geological Society of America Bulletin*, 115, 89–104.
- Cyz, M., Mulińska, M., Pachytel, R., Malinowski, M. 2018. Brittleness prediction for the Lower Paleozoic

- shales in northern Poland. *Interpretation*, 6 (3), 1–11, doi: 10.1190/int-2017-0203.1.
- De Vos, W., Pharaoh, T.C., Feldrappe, H., Smith, N. 2010. Pre-Devonian. Doornenbal, J.C., Stevenson, A.G. (eds), *Permian Basin Area*. Publisher: EAGE Publications b.v. (Houten), 59–69.
- Delabroye, A., Vecoli, M. 2010. The end-Ordovician glaciation and the Hirnantian Stage: A global review and questions about the Late Ordovician event stratigraphy. *Earth-Science Reviews*, 98 (3–4), 269–282, <https://doi.org/10.1016/j.earscirev.2009.10.010>.
- Dembicki, H. 2017. *Practical Petroleum Geochemistry for Exploration and Production. 1st Edition*, Elsevier. ISBN: 9780128033517.
- Finnegan, S. 2011. The Magnitude and Duration of the Late Ordovician-Early Silurian Glaciation. *Science*, 331 (6019), 903–906, doi: 10.1126/science.1200803.
- Freimanis, A., Margulis, L.S., Brangulis, A., Kanev, S., Pomerantseva, R. 1993. Geology and hydrocarbon prospects of Latvia. *Oil and Gas Journal* 6 (12), 71–74.
- Gamero-Diaz, H., Miller, C.M., Lweis, R. 2013. Score: A Mineralogy Based Classification Scheme for Organic Mudstones. *SPE Annual Technical Conference and Exhibition, 30 September – 2 October, New Orleans, Louisiana, USA, Society of Petroleum Engineers*, 1–13.
- Glorioso, J.C., Rattia, A. 2012. Unconventional Reservoirs: Basic Petrophysical Concepts for Shale Gas. In: *Proceedings of the SPE/EAGE European Unconventional Resources Conference and Exhibition from Potential to Production*, Vienna, Austria, 20–22 March 2012.
- Heasler, H.P., Kharitonova, N.A. 1996. Analysis of sonic well logs applied to erosion estimates in the Bighorn basin, Wyoming. *American Association of Petroleum Geologists Bulletin*, 80, 630–646.
- Horne, D.J. 1999. Ocean Circulation Modes of the Phanerozoic: Implications for the Antiquity of Deep-Sea Benthonic. *Crustaceana*, 72 (8), 999–1018.
- Horsfield, B., Schulz, H.-M., GASH Team. 2008. GASH: A shale gas initiative for Europe. EGU General Assembly. *Geophysical Research Abstracts*, 10, 1–2. EGU2008-A-01508.
- Jarvie, D.M., Hill, R.J., Ruble, T.E., Pollastro, R. 2007. Unconventional shale-gas systems: The Mississippian Barnett Shale of North-Central Texas as one model for thermogenic shale-gas assessment. *American Association of Petroleum Geologists Bulletin*, 91, 475–499, <https://doi.org/10.1306/12190606068>.
- Jarzyna, J.A., Bała, M., Krakowska, P.I., Puskarczyk, E., Strzempowicz, A., Wawrzyniak-Guz, K., Wieclaw, D., Ziętek J. 2017. Shale gas in Poland. *Advances in Natural Gas Emerging Technologies, Chapter 9*, INTECH, 191–210.
- Jin, X., Shah, S., Truax, J., Roegiers, J.C. 2014. A practical petrophysical approach for brittleness prediction from porosity and sonic logging in shale reservoirs. In: *Proceedings of the SPE Annual Technical Conference and Exhibition, Amsterdam, The Netherlands, 27–29 October 2014*.
- Magara, K. 1976. Thickness of removed sedimentary rocks, paleopore pressure, and paleotemperature, southwestern part of Western Canada Basin. *American Association of Petroleum Geologists Bulletin*, 60, 554.
- Kadūnienė, E. 1978. Distribution of the organic matter in the deposits of Caledonian geotectonic stage in the Baltic syncline. *Achievements and perspectives of the geological researches of the Lithuanian SSR*, Vilnius, 135–138.
- Kadūnienė, E. 2001. Organic matter in oil source rocks. In: Zdanavičiūtė, O., Sakalauskas, K. (eds) *Petroleum Geology of Lithuania and Southeastern Baltic*. Institute of Geology, Vilnius, 96–119.
- Kanev, S., Margulis, L., Bojesen-Koefoed, J.A., Weil, W.A., Merta, H., Zdanavičiūtė, O. 1994. Oil and hydrocarbon source rocks of the Baltic Syncline. *Oil and Gas Journal*, 92 (8), 69–73.
- Kias, E., Maharidge, R. Hurt, R. 2015. Mechanical versus mineralogical brittleness index across various shale plays. *Presented at the Annual Technical Conference and Exhibition, SPE, 174781*, <https://doi.org/10.2118/174781-MS>.
- Knoll, A.H., Holland, H.D. 1995. Oxygen and Proterozoic Evolution: An Update. In: *Board on Earth Sciences and Resources, Effects of Past Global Change on Life*. National Academy Press Washington, D.C., 1, 21–33.
- Lapinskas, P. 2000. *Structure and petroleum potential of the Silurian in Lithuania*. Institute of Geology, Vilnius, 203 pp.
- Laškovas, J. 2000. *Sedimentation Environments of the Ordovician Basin in the Southwestern Margin of the East European Platform and Lithogenesis of Deposits*. Institute of Geology, Vilnius, 314 pp.
- Lazauskienė, J., Stephenson, R.A., Šliaupa, S., Van Wees, J.-D. 2002. 3D flexural model of the Silurian Baltic Basin. *Tectonophysics*, 346, 115–135.
- Lazauskiene, J., Šliaupa, S., Musteikis, P., Brazauskas, A. 2003. Sequence stratigraphy of the Baltic Silurian succession: Tectonic control on the foreland infill. *Geological Society, London, Special Publications*, 208, 95–115.
- Loydell, D.K., Butcher, A., Frýda, J. 2013. The middle Rhuddanian (lower Silurian) ‘hot’ shale of North Africa and Arabia: An atypical hydrocarbon source rock. *Palaeogeography, Palaeoclimatology, Palaeoecology*, 386, 233–256.
- Lu, S.F., Wang, M., Xue, H.T. 2012. Classification and evaluation criteria of shale of shale oil and gas resources: discussion and application. *Petroleum Exploration and Development*, 39 (2), 268–276.
- Mandile, A.J., Hutton, A.C. 1995. Quantitative X-ray diffraction analysis of mineral and organic phases in organic-rich rocks. *International Journal of Coal Geology*, 28 (1), 51–69, [https://doi.org/10.1016/S0899-5362\(96\)00052-8](https://doi.org/10.1016/S0899-5362(96)00052-8).
- Moreau, J. 2011. The Late Ordovician deglaciation sequence of the SW. *Basin Research*, 23, 449–477.
- Motuz, G., Šliaupa, S., Timmerman, M.J. 2015. Geo-

- chemistry and $^{40}\text{Ar}/^{39}\text{Ar}$ age of Early Carboniferous dolerite sills in the southern Baltic Sea. *Estonian Journal of Earth Sciences*, 64 (3), 233–248, doi: 10.3176/earth.2015.30.
- Mystkowski, K., Srodon, J., McCarty, D.K. 2002. Application of evolutionary programming to automatic XRD quantitative analysis of clay-bearing rocks. *The Clay Minerals Society 39th Annual Meeting, Boulder, CO, Abstracts with Programs*.
- Pachytel, R.W., Jarosiński, M., Bobek, K. 2017. Geomechanical stratification in a shale reservoir and its correlation with natural fractures, Case from Pomeranian Basin (Poland). *51st U.S. Rock Mechanics/Geomechanics Symposium, ARMA*, 17–77.
- Passey, Q.R., Creaney, S., Kulla, J.B., Moretti, F.J., Stroud, J.D. 1990. A practical model for organic richness from porosity and resistivity logs. *American Association of Petroleum Geologists Bulletin*, 74 (12), 1777–1794.
- Paškevičius, J. 1997. *The geology of the Baltic Republics*. Geological Survey of Lithuania, Vilnius, 388 pp.
- Paškevičius, J. 2019. Zonation of Lithuanian Silurian graptolites and other faunal groups. *Geologija. Geografija*, 5 (2), 86–100.
- Perez, R., Marfurt, K. 2013. Brittleness estimation from seismic measurements in unconventional reservoirs: Application to the Barnett Shale. *SEG Technical Program Expanded Abstracts*, 75 (8), 172, doi: 10.1190/segam2013-0006.1.
- Peters, K.E., 1986. Guide lines for evaluating petroleum source rock using programmed pyrolysis. *American Association of Petroleum Geologists Bulletin*, 70, 318–329.
- Poprawa, P. 2010. Shale gas potential of the Lower Palaeozoic complex in the Baltic and Lublin-Podlasie basins (Poland) (in Polish). *Przegląd Geologiczny*, 58 (3), 226–249.
- Poprawa, P., Šliaupa, S., Stephenson, R.A., Lazauskienė, J. 1999. Late Ediacaran – Early Palaeozoic tectonic evolution of the Baltic basin: regional implications from subsidence analysis. *Tectonophysics*, 314, 219–239.
- Poprawa, P., Narkiewicz, M., Šliaupa, S., Stephenson, R., Lazauskienė, J. 1997. Caledonian accretion along TESZ. *Terra Nostra*, 11, 110–117.
- Poprawa, P., Šliaupa, S., Sidorov, V. 2006. Późnosylursko-wczesno dewońska śródpłytowa kompresja przed poluorogenu kaledońskiego (centralna częśćba senu bałtyckiego) – analiza danych sejsmicznych [Late Silurian – Early Devonian intra-plate compression in the foreland of the Caledonian orogen (central part of the Baltic Basin) – analysis of seismic data]. *Prace Państwowego Instytutu Geologicznego*, 186, 215–224.
- Rybacki, E.; Meier, T.; Dresen, G. 2016. What controls the mechanical properties of shale rocks? Part II: Brittleness. *Journal of Petroleum Science and Engineering*, 144, 39–58, doi: 10.1016/j.petrol.2016.02.022.
- Sondergeld, C.H., Newsham, K.E., Comisky, J.T., Rice, M.C. 2010. Petrophysical Considerations in Evaluating and Producing Shale Gas Resources. *Unconventional Gas Conference*, 23–25 February, Pittsburgh, Pennsylvania, USA, 1–34.
- Srodon, J., Drits, V.A., McCarty, D.K., Hsieh, J.C.C., Eberl, D.D. 2001. Quantitative X-ray diffraction analysis of clay-bearing rocks from random preparations. *Clays and Clay Minerals*, 49 (6), 514–528.
- Srodon, J., Elsass, E., McHardy, W.J., Morgan, D.J. 1992. Chemistry of illite-smectite inferred from TEM measurements of fundamental particles. *Clay Minerals*, 27, 137–158.
- Stirpeika, A. 1999. *Tectonic evolution of the Baltic syncline and local structures in the South Baltic region with respect to their petroleum potential*. Vilnius, 112 pp.
- Šliaupa, S. 1999. Far-field stress transmission indications in Early Palaeozoic structural evolution of the Baltic basin. *Romanian Journal of Tectonics and Regional Geology*, 77, 59.
- Šliaupa, S. 2002. Kinematic features of the Telšiai fault in Western Lithuania: structural and permeability prognosis. *Geologija*, 38, 24–30 [In Lithuanian with English summary].
- Šliaupa, S., Hoth, P. 2011. Geological evolution and resources of the Baltic Sea Area from the Precambrian to the Quaternary. In: Harff, J., Björck, S., Hoth, P. (eds), *The Baltic Sea Basin*. Springer, Berlin, 13–51, doi: 10.1007/978-3-642-17220-5_2.
- Šliaupa, S., Poprawa, P., Jacyna, J. 2000. Structural analysis of seismic data in the Baltic Basin: evidences for Silurian–Early Devonian intra-plate compression in the foreland of Caledonian orogen. *Journal of the Czech Geological Society*, 45, 3–4.
- Šliaupa, S., Hoth, P., Piske, J., Laskova, L., Bleschert, K-H. 2002. Burial history and maturation of Palaeozoic sediments between Rügen and Lithuania – conclusions for hydrocarbon exploration. *Proceedings of the 7th marine geological conference “Baltic-7” abstracts*, Kaliningrad, 119–120.
- Šliaupa, S., Laškovas, E., Lazauskienė, J., Laškova, L., Sidorov, V. 2004. The petroleum system of the Lithuanian offshore region. *Zeitschrift für Angewandte Geologie, Sonderheft 2*, 41–59.
- Šliaupa, S., Šliaupienė, R., Žaludienė, G., Vaskaboinikava, T., Bibikava, A., Evstratenko, L., Kovkhuto, A. 2016. Prospects of Lithuanian Silurian shale gas, Baltic sedimentary basin. *Oil Shale*, 33 (4), 357–372, doi: 10.3176/oil.2016.4.04.
- Šliaupa, S., Lozovskis, S., Lazauskienė, J., Šliaupienė, R. 2020. Petrophysical and mechanical properties of the lower Silurian perspective oil/gas shales of Lithuania. *Journal of Natural Gas Science and Engineering*, 79, <https://doi.org/10.1016/j.jngse.2020.103336>.
- Tassone, D.R., Holford, S., Duddy, S.R., Green, P.F., Hillis, R.R. 2014. Quantifying Cretaceous–Cenozoic exhumation in the Otway Basin, southeastern Australia, using sonic transit time data: implications for conventional and unconventional hydrocarbon prospectivity. *American Association of Petroleum Geologists Bulletin*, 98, 67, doi: 10.1306/04011312111.

- Thybo, H. 1997. Geophysical characteristics of the Tornquist Fan area, northwest Trans-European Suture Zone: Indication of late Carboniferous to early Permian dextral transtension. *Geological Magazine*, 134, 597–606.
- Tiryaki, B. 2006. Evaluation of the indirect measures of rock brittleness and fracture toughness in rock cutting: *The Journal of the South African Institute of Mining and Metallurgy*, 106, 407–423.
- Wang, F.P., Gale J.F. 2009. Screening criteria for shale-gas systems. *Gulf Coast Association of Geological Societies Transactions*, 59, 779–793.
- Wójcicki, A., Dyrka I., Kiersnowski, H., Adamczak-Bialy, T., Becker, A., Gluszyński, A., Janas, M., Karcz, P., Kozłowska, A., Kuberska, M., Paczeoena, J., Podhalańska, T., Skowroński, L., Waksmundzka, M.I. 2017. Prognostyczne zasoby gazu ziemnego i ropy naftowej w skałach łupkowych dolnego paleozoiku w basenie bałtycko-podlasko-lubelskimi w strefie Bilgoraj-Narol w Polsce) [Predictive natural gas and oil resources in the magnifying scales of the Lower Paleozoic in the Baltic-Podlasko-Lublin basin and in the Bilgoraj-Narol zone in Poland]. In: Wójcicki *et al.* (eds) *Szacowanie zasobów złóż węglowo dorów – zadanie ciągłe* ps. I etap Opracowanie końcowe: Inw. 9046/2019. NAG, State Geological Institute, Warsaw. [In Polish].
- Yasin, Q., Du, Q., Sohall, G., Atif, I. 2017. Impact of organic contents and brittleness indices to differentiate the brittle-ductile transitional zone in shale gas reservoir. *Geosciences Journal*, 21, 779–789, doi: 10.1007/s12303-017-0007-7.
- Zdanavičiūtė, O., Sakalauskas, K. (eds). 2001. *Petroleum geology of Lithuania and southeastern Baltic*. Geological Institute Publications, Vilnius, 204 pp.
- Zdanavičiūtė, O., Swadowska, E. 2002. Petrographic and pyrolysis-gas chromatography investigations of the Early Palaeozoic organic matter of Lithuania. *Geologija*, 40, 15–23.
- Zdanavičiūtė, O., Lazauskienė, J. 2007. The Petroleum potential of the Silurian succession in Lithuania. *Journal of Petroleum Geology*, 30 (4), 325–337.
- Zdanavičiūtė, O., Lazauskienė, J. 2009. Organic matter of Early Silurian succession – the potential source of unconventional gas in the Baltic Basin (Lithuania). *Baltica*, 22 (2), 89–98. ISSN 0067–3064.